Helsinki University of Technology Institute of Intelligent Power Electronics Publications
Espoo 2004 Publication 9

FLUX ESTIMATORS FOR SPEED-SENSORLESS INDUCTION MOTOR DRIVES

Thesis for the degree of Doctor of Science in Technology

Marko Hinkkanen

Dissertation for the degree of Doctor of Science in Technology to be presented with due permission of the Department of Electrical and Communications Engineering for public examination and debate in Auditorium S4 at Helsinki University of Technology (Espoo, Finland) on the 17th of September, 2004, at 12 noon.

Helsinki University of Technology
Department of Electrical and Communications Engineering
Power Electronics Laboratory

Teknillinen korkeakoulu
Sähkö- ja tietoliikennetekniikan osasto
Tehoelektroniikan laboratorio

Distribution:
Helsinki University of Technology
Power Electronics Laboratory
P.O. Box 3000
FIN-02015 HUT
Fax: +358-9-451 2432

ISBN 951-22-7189-3
ISBN 951-22-7188-5 (printed version)
ISSN 1456-0445

Espoo 2004

Abstract

This thesis deals with flux estimators for speed-sensorless induction motor drives. To enhance the stability and the performance of state-of-the-art sensorless drives, new flux estimator designs based on the standard motor model are proposed. Theoretical and experimental research methods are both used. The dynamics and stability of flux estimators are analyzed using linearized models, and the effects of parameter errors are investigated using steady-state relations. Performance is evaluated using computer simulations and laboratory experiments. It was found that most sensorless flux estimation methods proposed in the literature have an unstable operating region at low speeds (typically in the regenerating mode) and that the damping at high speeds may be insufficient. A new stable design of the speed-adaptive full-order flux observer is proposed: the observer gain is designed especially for nominal and high-speed operation, while the low-speed operation is stabilized by modifying the speed-adaptation law. Compared to estimators proposed in the literature, the effects of parameter errors on the proposed observer design are shown to be small. To further improve the robustness, the speed-adaptive observer is enhanced with a low-frequency signal-injection method, allowing long-term zero-frequency operation under rated load torque. Furthermore, a computationally efficient version of a voltage-model-based flux estimator and two computationally efficient digital implementations for full-order flux observers are proposed.

Index terms: Flux estimation, induction motor, sensorless control.

Preface

This work was carried out in the Power Electronics Laboratory at Helsinki University of Technology. It is part of a research project concerning sensorless control of ac motor drives. The work has been financed in part by ABB Oy and in part by the Graduate School in Electronics, Telecommunications and Automation (GETA).

Most of all, I would like to thank my supervisor Prof. Jorma Luomi for his encouragement, guidance, and support during this work. Furthermore, his constructive and precise comments on my manuscripts were always invaluable. I would also like to thank all those who were my colleagues during this work. Besides being an inexhaustible source of ideas, Dr. Veli-Matti Leppänen gave his contribution to the experimental setup used in this work and co-authored one of the publications. I also greatly enjoyed working with Mr. Petri Mäki-Ontto and Dr. Vesa Tuomainen, as well as with my more recent colleagues Mr. Antti Piippo, Mr. Janne Salomäki, and Mr. Henri Kinnunen. Prof. Jorma Kyyrä and Prof. Seppo Ovaska kindly answered my questions relating to power electronics and signal processing, respectively. Thanks are also due to our laboratory technician Mr. Ilkka Hanhivaara and our secretary Mrs. Anja Meuronen.

I am obliged to the people from ABB Oy who participated in the project. Discussions with Mr. Samuli Heikkilä, Mr. Mikko Vertanen, and Mr. Jukka Mustonen were especially helpful. Mr. Vesa Metso and Mr. Panu Virolainen made an important contribution relating to our experimental setup. I also owe my thanks to Mr. Matti Kauhanen, Mr. Mikko Korpinen, and Mr. Pasi Karhinen for organizing the project on behalf of ABB Oy.

The additional financial support given by the Finnish Society of Electronics Engineers, the Foundation of Technology, and the Finnish Cultural Foundation is gratefully acknowledged.

Finally, I would like to thank my wife Päivi for her love and support, and our five-month-old son Eetvi for his big smiles.

Espoo, August 2004

Marko Hinkkanen

Contents

List of Publications

This thesis consists of an overview and the following publications:

I Hinkkanen, M. and Luomi, J. (2003). "Modified integrator for voltage model flux estimation of induction motors." *IEEE Trans. Ind. Electron.*, **50**(4), pp. 818–820.

II Hinkkanen, M. and Luomi, J. (2002). "Zero-speed operation of sensorless induction motors using full-order flux observer." In *Proc. NORPIE/2002*, Stockholm, Sweden, CD-ROM.

III Hinkkanen, M. and Luomi, J. (2002). "Digital implementation of full-order flux observers for induction motors." In *Proc. EPE-PEMC'02*, Cavtat and Dubrovnik, Croatia, CD-ROM.

IV Hinkkanen, M. and Luomi, J. (2003). "Parameter sensitivity of full-order flux observers for induction motors." *IEEE Trans. Ind. Applicat.*, **39**(4), pp. 1127–1135.

V Hinkkanen, M. (2004). "Analysis and design of full-order flux observers for sensorless induction motors." *IEEE Trans. Ind. Electron.*, **51**(5), in press.

VI Hinkkanen, M. and Luomi, J. (2004). "Stabilization of regenerating-mode operation in sensorless induction motor drives by full-order flux observer design." *IEEE Trans. Ind. Electron.*, **51**(6), in press.

VII Hinkkanen, M., Leppänen, V.-M., and Luomi, J. (2005). "Flux observer enhanced with low-frequency signal injection allowing sensorless zero-frequency operation of induction motors." *IEEE Trans. Ind. Applicat.*, **41**(1), in press.

The author has written Publications I...VI with help and guidance from Prof. Luomi. Publication VII was written by the author, except the parts introducing and describing the signal-injection method written by Dr. Leppänen. Prof. Luomi and Dr. Leppänen helped in writing the final text of Publication VII. Dr. Leppänen also helped to implement the signal-injection part of the control algorithm used in Publication VII. The author is responsible for the analysis, simulations, and experiments.

Preliminary versions of Publications I, IV...VII were presented at conferences (Hinkkanen and Luomi, 2001, 2002, 2003; Hinkkanen, 2002a; Hinkkanen et al., 2003). A patent application (Hinkkanen, 2002b) corresponds to Publication VI.

Symbols

$\underline{\mathbf{A}}$, $\mathbf{B}$, $\mathbf{C}$	matrices of state-space representation
$\underline{e}_f$	flux-emf vector
$\underline{\mathbf{F}}$, $\mathbf{G}$, $\mathbf{H}$	matrices of state-space representation
$\underline{i}_r$	rotor current vector (T model)
$\underline{i}_R = \underline{i}_r/k_r$	rotor current vector (inverse-Γ model)
$\underline{i}_s$	stator current vector
i_{sa}, i_{sb}, i_{sc}	phase currents
i_{sd}, i_{sq}	real and imaginary components of $\underline{i}_s$
j	imaginary unit
J	total moment of inertia
$k_r = L_m/L_r$	magnetic coupling factor of rotor (not related to $\underline{k}_r$)
$\underline{\mathbf{K}} = [\underline{k}_s \quad \underline{k}_r]^T$	observer gain
$\underline{\mathbf{L}} = [\underline{l}_s \quad \underline{l}_r]^T$	observer gain
L_m	magnetizing inductance (T model)
$L_M = k_r L_m$	magnetizing inductance (inverse-Γ model)
L_r	rotor inductance
$L_{r\sigma}$	rotor leakage inductance
L_s	stator inductance
$L'_s = L_{s\sigma} + k_r L_{r\sigma}$	stator transient inductance
$L_{s\sigma}$	stator leakage inductance
p	number of pole pairs
R_r	rotor resistance (T model)
$R_R = k_r^2 R_r$	rotor resistance (inverse-Γ model)
R_s	stator resistance
t	time
T_e	electromagnetic torque
T_L	load torque
u_{dc}	dc-link voltage
$\underline{u}_s$	stator voltage vector

$\underline{\mathbf{x}} = [\underline{\psi}_s \quad \underline{\psi}_R]^T$	state vector of state-space representation
$\underline{\mathbf{z}} = [\underline{i}_s \quad \underline{\psi}_R]^T$	state vector of state-space representation
γ_p, γ_i	gains of speed-adaptation law
ε	error term of speed-adaptation law
ϑ_k	angle of general reference frame
ϑ_s	angle of rotor flux reference frame
$\sigma = L'_s/(L_M + L'_s)$	total leakage factor
$\tau_r = L_M/R_R$	rotor time constant
$\tau'_r = \sigma L_M/R_R$	transient rotor time constant
$\tau'_s = L'_s/R_s$	transient stator time constant
$\tau'_\sigma = L'_s/(R_s + R_R)$	time constant
$\underline{\psi}_r$	rotor flux linkage vector (T model)
$\underline{\psi}_R = k_r \underline{\psi}_r$	rotor flux linkage vector (inverse-Γ model)
$\underline{\psi}_s$	stator flux linkage vector
ω_k	angular speed of general reference frame
ω_m	electrical angular speed of rotor
$\omega_r = \omega_s - \omega_m$	angular slip frequency
ω_s	angular frequency of rotor flux (corresponds to angular stator frequency in steady state)

Complex-valued variables are underlined and complex conjugates are marked by the symbol *. Magnitudes of complex-valued variables are referred to by omitting the underlining, e.g., $|\underline{\psi}_R| = \psi_R$. Matrix transposes are marked by the symbol ^{T} and estimates are marked by the symbol $\hat{}$. Reference values are marked by the subscript ref.

Chapter 1

Introduction

Three-phase induction motors are the most widely used electrical motors, due to their ruggedness and low price. The induction motor can be operated directly from the mains, but variable speed and often better energy efficiency are achieved by means of a frequency converter between the mains and the motor. A typical frequency converter consists of a rectifier, a voltage-stiff dc link, and a pulse-width modulated (PWM) inverter. The inverter is controlled using a digital signal processor.

A simple way of controlling the induction motor is to adjust the magnitude of the stator voltage proportionally to a reference frequency (Schönung and Stemmler, 1964). This open-loop method, known as the scalar control or the constant voltage-per-hertz control, is still used in low-cost frequency converters due to its important advantages. A speed sensor (which is expensive, fragile, and requires extra cabling) is not needed. The knowledge of motor parameters is not necessary either, implying that the method is robust. In addition, a scalar controlled frequency converter can feed several motors connected in parallel. However, the dynamic performance and the speed accuracy are poor, even if compensation for the stator resistance voltage drop and a slip compensation are used. Furthermore, oscillations at light loads may occur (Nelson et al., 1969).

The rotor flux orientation control by Blaschke (1972) made it possible to use induction motors in applications requiring high-performance torque and speed control. In the reference frame fixed to the direction of the rotor flux, the flux- and torque-producing current components can be controlled separately, resembling the control of dc motors. The rotor flux, whose angle is needed for coordinate transformations between the stationary and rotor flux reference frames, can be estimated with good accuracy if a speed sensor is used (Bauer and Heining, 1989).

The controller's reference frame can also be fixed to the stator flux estimate (Xu and Novotny, 1991). The stator flux orientation control is more complicated than the rotor flux orientation control, but the flux estimation is slightly simpler if the estimator uses only the stator dynamics. In the direct torque control (DTC) proposed by Takahashi and Noguchi (1986) and Depenbrock (1988), the switching functions are directly generated on the basis of the estimates of the stator flux and the electromagnetic torque. Flux orientation control methods and the direct torque control can be classified as vector control methods.

Advances in digital signal processors started the development of speed-sensorless vector control in the late 1980s. In spite of research carried out for more than a decade, state-of-the-art sensorless drives still suffer from degraded performance and unstable operating regions at low speeds. The main reason for the stability problems is the difficulty of flux estimation without speed measurement.

Conventional speed-sensorless flux estimators, such as the voltage model (Takahashi and Noguchi, 1986) and the speed-adaptive full-order flux observer (Kubota et al., 1993), are based on the standard dynamic motor model. Performance comparable to that of drives equipped with the speed sensor can be achieved in a wide speed and load range. However, it is well known that methods based on the standard motor model have fundamental problems at very low frequencies. In the vicinity of zero frequency, estimation is very sensitive to errors in measurements and the stator resistance estimate. At zero stator frequency, the flux and the speed are unobservable from the stator current and voltage.

Furthermore, the flux estimator and the motor dynamics together form a nonlinear closed-loop system through the coordinate transformations (Harnefors, 2001). Even if the flux estimator itself is simple, the nonlinear closed-loop system is typically complicated. Problems can therefore also be encountered at higher speeds, unless the estimator is properly designed. For example, the system may become poorly damped or sluggish at very high speeds, causing degraded dynamic performance. As stated by Verghese and Sanders (1988), computationally efficient digital implementation is also a challenge at high speeds.

To improve the robustness of sensorless drives at low speeds, estimators based on a spatial magnetic or electric anisotropy of the motor have been developed. A high-frequency voltage signal, superimposed on the fundamental voltage, is typically used to excite the anisotropic phenomena of the motor; the rotor position or the flux direction is identified from the current response. Most of the signal-injection methods require a spatial variation of the leakage inductance that is linked to the rotor position (Jansen and Lorenz, 1995), or flux direction (Jansen and Lorenz, 1996). Instead of an additional test signal, Schroedl (1996) and Holtz et al. (1997) use the PWM switching waveform for the excitation.

Unfortunately, signal-injection methods based on spatially anisotropic models have several well-known problems (Leppänen, 2003). Anisotropies depend on the motor design, and they are usually weak in standard induction motors. A signal carrying useful information is generally corrupted by other signals of the same kind. Furthermore, the spatial variation of the leakage inductance depends on load and flux level, often leading to difficulties at high loads. To circumvent the aforementioned problems, a low-frequency current-signal injection was recently proposed by Leppänen and Luomi (2002). The low-frequency signal-injection method uses the response of the mechanical system, and is based on the standard motor model. The method exhibits good steady-state performance down to zero-frequency operation, and is insensitive to parameter errors, provided that the total moment of inertia is not too high. A common drawback of signal-injection methods is that their dynamic response is usually only moderate.

The goal of this thesis is to develop a speed-sensorless flux estimator with the following properties:

- Usable with a standard off-the-shelf induction motor.
- Allows high dynamic performance of the system.
- Allows robust four-quadrant operation from zero speed up to very high speeds.
- Requires only the stator current and dc-link voltage measurements.
- Digital implementation is computationally efficient.

This thesis focuses on methods based on the standard motor model. The rotor flux orientation control, popular among both academic and industrial communities, is used. Methods

using soft computing (e.g., neural networks or fuzzy systems) or Kalman filtering are beyond the scope of this thesis.

This thesis consists of an overview and seven Publications, numbered corresponding to the chronological order of their conference versions. This overview is organized as follows. Chapter 2 presents the mathematical model of the induction motor, while Chapter 3 reviews the most interesting sensorless flux estimators proposed in the literature. Chapter 4 describes the experimental setup used to obtain the experimental results of the Publications; Chapter 5 summarizes the Publications and Chapter 6 concludes the thesis.

Chapter 2

System Model

2.1 Space Vectors

The space vector approach by Kovács and Rácz (1959a) is commonly used to model the dynamic behaviour of ac machines. The space vector is a complex variable, whose amplitude and angle can vary arbitrarily in time. The current is assumed to be distributed sinusoidally along the air gap. The space vector of the stator current in the stator reference frame is defined by

$$\underline{i}_s = \frac{2}{3}\left(i_{sa} + i_{sb}e^{j2\pi/3} + i_{sc}e^{j4\pi/3}\right) \tag{2.1}$$

where i_{sa}, i_{sb}, and i_{sc} are the phase currents. If zero-sequence components exist, they have to be treated separately. The definition of the zero-sequence current is

$$i_{s0} = \frac{1}{3}\left(i_{sa} + i_{sb} + i_{sc}\right) \tag{2.2}$$

In practice, zero-sequence currents do not exist since the stator winding is delta-connected or the star point is not connected. The phase currents are obtained using relations

$$i_{sa} = \mathrm{Re}\left\{\underline{i}_s\right\} + i_{s0} \tag{2.3a}$$
$$i_{sb} = \mathrm{Re}\left\{\underline{i}_s e^{j4\pi/3}\right\} + i_{s0} \tag{2.3b}$$
$$i_{sc} = \mathrm{Re}\left\{\underline{i}_s e^{j2\pi/3}\right\} + i_{s0} \tag{2.3c}$$

Coordinate transformations between the stator reference frame and the general reference frame (indicated by superscript k) are

$$\underline{i}_s^k = \underline{i}_s e^{-j\vartheta_k} \tag{2.4a}$$
$$\underline{i}_s = \underline{i}_s^k e^{j\vartheta_k} \tag{2.4b}$$

where ϑ_k is the angle of the general reference frame. No superscript indicating the reference frame is used if the reference frame appears from the context. The real and imaginary components of the stator current vector[1] correspond to $\underline{i}_s = i_{sd} + ji_{sq}$. The space vectors of other currents, voltages, and flux linkages are defined similarly.

[1]The notation $\underline{i}_s = i_{s\alpha} + ji_{s\beta}$ is also used in the stator reference frame.

2.2 Induction Motor

Two mathematically equal flux linkage models of the induction motor are shown in Fig. 2.1. The conventional T model is commonly used in the literature but the simpler inverse-Γ model is more suitable for control purposes.

T Model

The voltage equations of the induction motor are in a general reference frame (Kovács and Rácz, 1959b)

$$\underline{u}_s = R_s \underline{i}_s + \frac{d\underline{\psi}_s}{dt} + j\omega_k \underline{\psi}_s \tag{2.5a}$$

$$0 = R_r \underline{i}_r + \frac{d\underline{\psi}_r}{dt} + j\left(\omega_k - \omega_m\right)\underline{\psi}_r \tag{2.5b}$$

where $\underline{u}_s$ is the stator voltage, R_s the stator resistance, $\underline{i}_s$ the stator current, and ω_k the angular speed of the reference frame. The rotor resistance is R_r, the rotor current $\underline{i}_r$, and the electrical angular speed of the rotor ω_m. The stator and rotor flux linkages are

$$\underline{\psi}_s = L_s \underline{i}_s + L_m \underline{i}_r \tag{2.6a}$$

$$\underline{\psi}_r = L_m \underline{i}_s + L_r \underline{i}_r \tag{2.6b}$$

respectively, where L_m, L_s, and L_r are the magnetizing inductance, the stator inductance, and the rotor inductance, respectively. The stator and rotor inductances are defined by $L_s = L_m + L_{s\sigma}$ and $L_r = L_m + L_{r\sigma}$, respectively, where $L_{s\sigma}$ and $L_{r\sigma}$ are the stator and rotor leakage inductances, respectively. The flux linkage model corresponding to (2.6) is shown in Fig. 2.1(a).

The electromagnetic torque is given by

$$T_e = \frac{3}{2} p \,\mathrm{Im}\left\{\underline{i}_s \underline{\psi}_s^*\right\} \tag{2.7}$$

where the number of pole pairs is p and the complex conjugate is marked by the symbol *. The equation of motion is

$$\frac{d\omega_m}{dt} = \frac{p}{J}\left(T_e - T_L\right) \tag{2.8}$$

where the total moment of inertia of the mechanical system is J and the load torque is T_L.

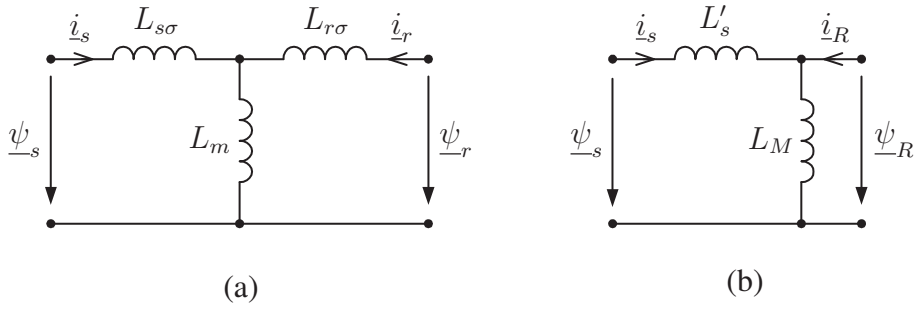

Figure 2.1. Flux linkage models: (a) T model; (b) inverse-Γ model.

Inverse-Γ Model

As shown by Slemon (1989), the number of model parameters can be decreased from five to four by scaling the rotor flux linkage $\underline{\psi}_R = k_r \underline{\psi}_r$ and the rotor current $\underline{i}_R = \underline{i}_r / k_r$, where the magnetic coupling factor of the rotor is defined by $k_r = L_m / L_r$. Furthermore, the scaled magnetizing inductance $L_M = k_r L_m$, the scaled rotor resistance $R_R = k_r^2 R_r$, and the stator transient inductance $L'_s = L_{s\sigma} + k_r L_{r\sigma}$ are introduced. Now the voltage equations (2.5) become

$$\underline{u}_s = R_s \underline{i}_s + \frac{d\underline{\psi}_s}{dt} + j\omega_k \underline{\psi}_s \tag{2.9a}$$

$$0 = R_R \underline{i}_R + \frac{d\underline{\psi}_R}{dt} + j\left(\omega_k - \omega_m\right) \underline{\psi}_R \tag{2.9b}$$

and the flux linkage equations corresponding to (2.6) are

$$\underline{\psi}_s = \left(L'_s + L_M\right) \underline{i}_s + L_M \underline{i}_R \tag{2.10a}$$

$$\underline{\psi}_R = L_M \left(\underline{i}_s + \underline{i}_R\right) \tag{2.10b}$$

The flux linkage model corresponding to (2.10) is shown in Fig. 2.1(b). Equations (2.7) and (2.8) remain unchanged for the inverse-Γ model. The inverse-Γ model will be exclusively used in this thesis.

State-Space Representations and Flux-EMF

When the stator flux and the rotor flux are chosen as state variables, the state-space representation of (2.9) and (2.10) becomes

$$\frac{d\underline{\mathbf{x}}}{dt} = \underbrace{\begin{bmatrix} -\frac{1}{\tau'_s} - j\omega_k & \frac{1}{\tau'_s} \\ \frac{1-\sigma}{\tau'_r} & -\frac{1}{\tau'_r} - j\left(\omega_k - \omega_m\right) \end{bmatrix}}_{\underline{\mathbf{A}}} \underline{\mathbf{x}} + \underbrace{\begin{bmatrix} 1 \\ 0 \end{bmatrix}}_{\mathbf{B}} \underline{u}_s \tag{2.11a}$$

$$\underline{i}_s = \underbrace{\begin{bmatrix} \frac{1}{L'_s} & -\frac{1}{L'_s} \end{bmatrix}}_{\mathbf{C}} \underline{\mathbf{x}} \tag{2.11b}$$

where the state vector is $\underline{\mathbf{x}} = [\underline{\psi}_s \quad \underline{\psi}_R]^T$, the total leakage factor is $\sigma = L'_s / (L_M + L'_s)$, the transient stator time constant is $\tau'_s = L'_s / R_s$, and the transient rotor time constant is $\tau'_r = \sigma L_M / R_R$. Another useful representation is obtained using the stator current and the rotor flux as state variables, leading to

$$\frac{d\underline{\mathbf{z}}}{dt} = \underbrace{\begin{bmatrix} -\frac{1}{\tau'_\sigma} - j\omega_k & \frac{1}{L'_s}\left(\frac{1}{\tau_r} - j\omega_m\right) \\ R_R & -\frac{1}{\tau_r} - j\left(\omega_k - \omega_m\right) \end{bmatrix}}_{\underline{\mathbf{F}}} \underline{\mathbf{z}} + \underbrace{\begin{bmatrix} \frac{1}{L'_s} \\ 0 \end{bmatrix}}_{\mathbf{G}} \underline{u}_s \tag{2.12a}$$

$$\underline{i}_s = \underbrace{\begin{bmatrix} 1 & 0 \end{bmatrix}}_{\mathbf{H}} \underline{\mathbf{z}} \tag{2.12b}$$

where the state vector is $\underline{\mathbf{z}} = [\underline{i}_s \quad \underline{\psi}_R]^T$, a time constant is $\tau'_\sigma = L'_s / (R_s + R_R)$, and the rotor time constant is $\tau_r = L_M / R_R$.

For future reference, the flux-emf is defined by

$$\underline{e}_f = \frac{d\underline{\psi}_R}{dt} + j\omega_k \underline{\psi}_R \tag{2.13}$$

Using (2.9) and (2.10), the flux-emf can be expressed by the stator current and the rotor flux in the following forms:

$$\underline{e}_f = \underline{u}_s - R_s \underline{i}_s - L'_s \frac{d\underline{i}_s}{dt} - j\omega_k L'_s \underline{i}_s \tag{2.14}$$

$$\underline{e}_f = \left(-\frac{1}{\tau_r} + j\omega_m \right) \underline{\psi}_R + R_R \underline{i}_s \tag{2.15}$$

corresponding to the stator and rotor equations, respectively. Two conventional flux estimators, the voltage model and the current model, are based on (2.14) and (2.15), respectively.

2.3 Rotor Flux Orientation

The principle of rotor flux orientation is briefly described here. The reference frame fixed to the actual rotor flux is considered, i.e.,

$$\omega_k = \omega_s, \quad \underline{\psi}_R = \psi_R + j0 \tag{2.16}$$

where ω_s is the angular speed of the rotor flux. Based on (2.13), (2.15), and (2.16), the dynamics of the rotor flux and the slip relation can be written

$$\frac{d\psi_R}{dt} = -\frac{1}{\tau_r}\psi_R + R_R i_{sd} \tag{2.17}$$

$$\omega_r = \frac{R_R i_{sq}}{\psi_R} \tag{2.18}$$

respectively, where the angular slip frequency is $\omega_r = \omega_s - \omega_m$. Using (2.10) and (2.16), the expression for the electromagnetic torque (2.7) in the rotor flux reference frame reduces to

$$T_e = \frac{3}{2} p \psi_R i_{sq} \tag{2.19}$$

According to (2.17) and (2.19), the d and q components of the stator current can be used to control the rotor flux magnitude and the electromagnetic torque, respectively.

2.4 Operating Modes

Three operating modes of the induction motor are defined here based on the signs of the air-gap power p_δ and the mechanical power p_m. The air-gap power transferred into the rotor can be expressed as

$$\begin{aligned} p_\delta &= -\frac{3}{2}\,\mathrm{Re}\{\underline{e}_f \underline{i}_R^*\} \\ &= \frac{3}{2}\left[\frac{1}{R_R}\left(\frac{d\psi_R}{dt}\right)^2 + \frac{\psi_R^2\omega_s^2}{R_R}\frac{\omega_r}{\omega_s}\right] \end{aligned} \tag{2.20}$$

where ω_s is the angular speed of the rotor flux. In steady state, the air-gap power is negative only if the relative slip is $\omega_r/\omega_s < 0$. The mechanical power

$$\begin{aligned} p_m &= T_e\frac{\omega_m}{p} \\ &= \frac{3}{2}\frac{\psi_R^2\omega_s^2}{R_R}\left(\frac{\omega_r}{\omega_s} - \frac{\omega_r^2}{\omega_s^2}\right) \end{aligned} \tag{2.21}$$

is positive only if $0 < \omega_r/\omega_s < 1$. Based on the equations, the operating modes of the induction motor can be defined as (Leonhard, 1996):

1. regenerating mode ($\omega_r/\omega_s < 0$);
2. motoring mode ($0 < \omega_r/\omega_s < 1$);
3. plugging mode ($\omega_r/\omega_s > 1$).

To recognize the plugging (braking) mode more easily, the condition for it can also be expressed as $\omega_m\omega_s < 0$.

Chapter 3

Sensorless Flux Estimation

This chapter reviews speed-sensorless flux estimation methods proposed in the literature. To provide a background, examples of sensorless rotor flux orientation control systems are firstly described in Section 3.1. Then, sensorless flux estimators based on the standard motor model are discussed. The estimators can be divided into two main groups: inherently sensorless flux estimators (Section 3.2) and speed-adaptive flux estimators (Sections 3.3 and 3.4). Inherently sensorless flux estimators are independent of the rotor speed estimation (but the speed estimation is based on the flux estimation), whereas the flux estimation and the speed estimation are coupled in speed-adaptive flux estimators.

Both approaches are widely used and have their own merits. Inherently sensorless methods require typically less computation whereas the speed-adaptation mechanism seems to imply tolerance of measurement noise. The flexibility of the speed-adaptive full-order flux observer structure is tempting: the same analysis tools and experimental algorithms can be used for different observer designs.

The dynamics of sensorless flux estimators and the actual motor are generally coupled through the coordinate transformations (Harnefors, 2001). The nonlinear closed-loop system consisting of the flux estimator and the motor can be studied via small-signal linearization in a synchronous reference frame. Unless otherwise noted, the comments on the dynamics and the stability in this chapter are based on the linearization analysis and computer simulations carried out by the author. The linearization method proposed by Harnefors (2001) is used for inherently sensorless flux estimators, and the linearized model for speed-adaptive full-order flux observers can be found in Publication V. Accurate motor parameter estimates have been assumed in the linearized models.

To make the comparison of estimators easier, they are considered mainly in the general reference frame, and the rotor flux orientation control is assumed. Parameter errors, online estimation of the stator resistance, and flux estimators combined with signal injection are briefly discussed in Sections 3.5, 3.6, and 3.7, respectively.

3.1 Control System

Speed-sensorless flux estimators operate within the framework of sensorless control. Two typical sensorless rotor flux orientation control systems are depicted in Fig. 3.1 as examples. In Fig. 3.1(a), the flux estimator is implemented in the stator reference frame, where the angular frequency of the reference frame and the rotor flux estimate are

$$\omega_k = 0, \quad \underline{\hat{\psi}}_R = \hat{\psi}_R e^{j\hat{\vartheta}_s} \tag{3.1}$$

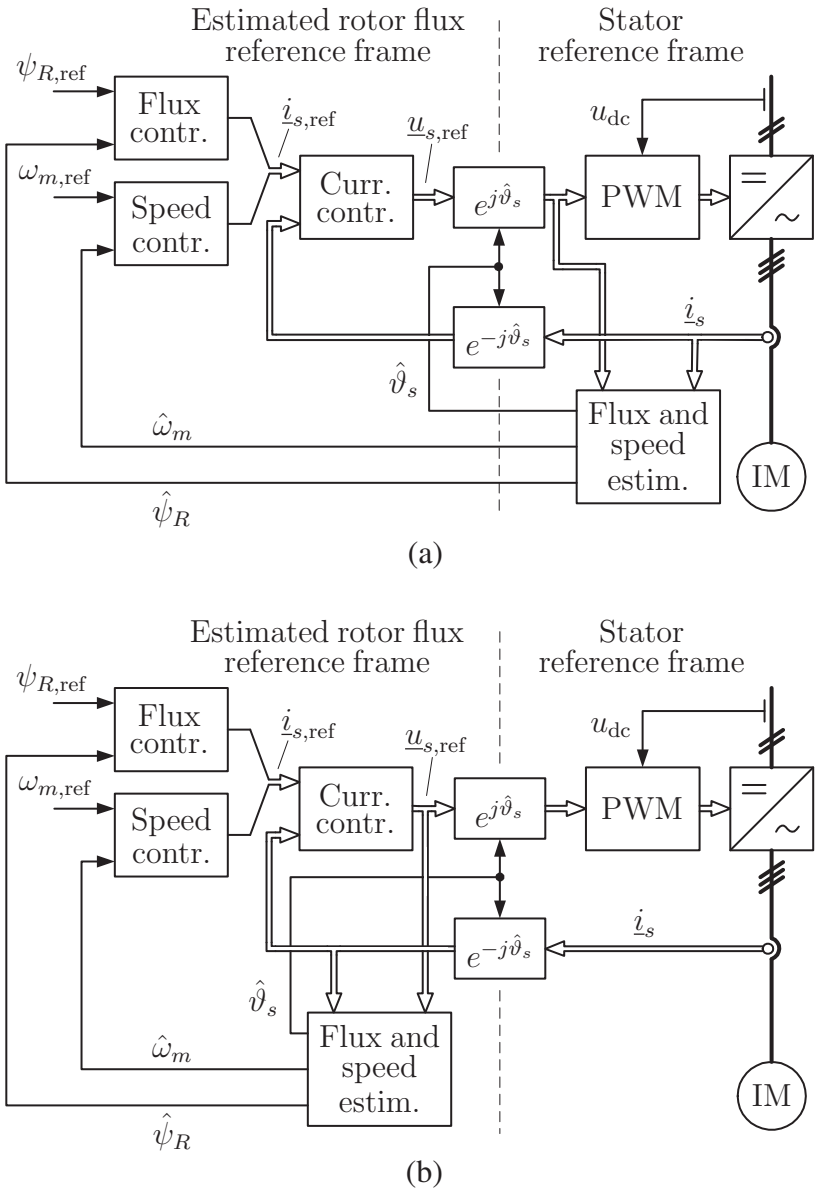

Figure 3.1. Rotor flux orientation control. Flux estimation in (a) stator reference frame and (b) in estimated rotor flux reference frame. Space vectors shown on left-hand side of coordinate transformations are in the estimated rotor flux reference frame and space vectors on right-hand side are in the stator reference frame.

respectively. The angle of the rotor flux estimate is denoted by $\hat{\vartheta}_s$ and can be calculated from the components of $\underline{\hat{\psi}}_R$, e.g., using the arctan function. The angular frequency $\hat{\omega}_s$ of the estimated rotor flux[1] can be obtained by differentiating $\hat{\vartheta}_s$. In steady state, the electrical variables vary sinusoidally in time with angular stator frequency. Therefore, digital implementation of flux estimators in the stator reference frame may become inaccurate or unstable at high speeds as described in Publication III.

In Fig. 3.1(b), the flux estimator is implemented in the estimated rotor flux reference frame, where

$$\omega_k = \hat{\omega}_s, \quad \underline{\hat{\psi}}_R = \hat{\psi}_R + j0 \tag{3.2}$$

As discussed in Publication IV, an algebraic relation for the angular frequency $\hat{\omega}_s$ can be

[1]The angular frequency of the estimated rotor flux is denoted by ω_s in Publications I. . . VI.

obtained for a flux estimator under consideration using (3.2). The angle $\hat{\vartheta}_s$ is obtained by integrating $\hat{\omega}_s$. In steady state, the electrical variables are constant in the estimated rotor flux reference frame. Consequently, the accuracy of digital implementation is usually sufficient, but the stability problems at high speeds may occur if the forward Euler discretization is used as shown in Publication III.

The stator current $\underline{i}_s$ and the dc-link voltage u_{dc} are measured and used as feedback variables in the controller. Based on the stator voltage reference $\underline{u}_{s,\mathrm{ref}}$ and the dc-link voltage, the pulse-width modulator (PWM) generates the switching functions for the power semiconductor switches of the inverter (e.g., Holtz, 1994). The stator voltage reference is used in the flux estimator, i.e., the stator voltage $\underline{u}_s$ is assumed to equal its reference. This assumption holds well if the inverter nonlinearities, mainly caused by the dead-time effect and power device voltage drops, are compensated (Publication II and references therein). The compensation is especially important at low stator frequencies since the amplitude of the fundamental-wave stator voltage is low. The compensation of inverter nonlinearities is not presented in Fig. 3.1

The voltage reference $\underline{u}_{s,\mathrm{ref}}$ is the output of the synchronous-frame PI-type current controller augmented with a feedforward back-emf compensation (e.g., Briz et al., 2000). The tuning of the synchronous-frame current controller is discussed by Harnefors and Nee (1998). The real and imaginary components of the current reference $\underline{i}_{s,\mathrm{ref}} = i_{sd,\mathrm{ref}} + j i_{sq,\mathrm{ref}}$ are the flux and speed controller outputs, respectively. The flux and speed controllers are usually PI-type controllers, the flux controller possibly augmented with a feedforward path (Briz et al., 2001). The flux controller can be omitted if field-weakening operation is not required. Then $i_{sd,\mathrm{ref}} = \psi_{R,\mathrm{ref}}/\hat{L}_M$ is selected, where $\psi_{R,\mathrm{ref}}$ is the rotor flux reference and $\hat{L}_M$ is the magnetizing inductance estimate. The speed reference is denoted by $\omega_{m,\mathrm{ref}}$ and the speed estimate by $\hat{\omega}_m$. For simplicity, signals corresponding to feedforward paths, limitation, or the anti-windup of controllers are not drawn in Fig. 3.1.

The controllers are usually designed to operate in different time scales (Harnefors, 1997). The current control loop is the fastest control loop, its bandwidth corresponding approximately to one tenth of the angular sampling frequency. The speed control loop is usually at least as fast as the flux control loop. The dynamics of the flux and speed estimator (or more accurately, the closed-loop dynamics of the estimator and the actual flux) should be considerably faster than the flux and speed control loops.

3.2 Inherently Sensorless Flux Estimators

Pure Voltage Model

The voltage model was proposed by Takahashi and Noguchi (1986) and Depenbrock (1988) in connection with direct torque control. Xu and Novotny (1991) applied the voltage model in stator flux orientation control, while Ohtani et al. (1992), for example, used a modified voltage model in rotor flux orientation control.

For the rotor flux estimate, the voltage model can be written from (2.13) and (2.14) in the general reference frame as

$$\frac{d\hat{\underline{\psi}}_R}{dt} = \underbrace{\underline{u}_s - \hat{R}_s \underline{i}_s - \hat{L}'_s \frac{d\underline{i}_s}{dt} - j\omega_k \hat{L}'_s \underline{i}_s}_{\hat{\underline{e}}_f} - j\omega_k \hat{\underline{\psi}}_R \tag{3.3}$$

where $\hat{R}_s$ is the stator resistance estimate and $\hat{L}'_s$ is the stator transient inductance estimate. Furthermore, the estimate $\hat{\underline{e}}_f$ of the flux-emf is defined in (3.3) in order to shorten the following equations. As can be seen, the rotor speed is not included in the voltage model.

Based on (2.18), the rotor speed can be estimated as (e.g., Schauder, 1992)

$$\hat{\omega}_m = \mathrm{LPF}\left\{\hat{\omega}_s - \frac{\hat{R}_R i_{sq}}{\hat{\psi}_R}\right\} \tag{3.4}$$

where $\hat{\omega}_s$ is the angular frequency of the estimated rotor flux, i_{sq} is the q component of the stator current in the estimated rotor flux reference frame, $\hat{\psi}_R$ is the magnitude of the estimated rotor flux, and $\hat{R}_R$ is the rotor resistance estimate. In practice, low-pass filtering (LPF) of the speed estimate is necessary. If another reference frame is preferred, (3.4) can be generalized as

$$\hat{\omega}_m = \mathrm{LPF}\left\{\hat{\omega}_s - \frac{\hat{R}_R \,\mathrm{Im}\{\underline{i}_s \hat{\underline{\psi}}_R^*\}}{\hat{\psi}_R^2}\right\} \tag{3.5}$$

The dynamics of the closed-loop system consisting of an inherently sensorless flux estimator and the motor generally differ from the dynamics of the estimator only. The pure voltage model is an exception: the poles of both the estimator (3.3) and the corresponding linearized closed-loop system are on the imaginary axis (Harnefors, 2001). The system is only marginally stable and the damping is thus insufficient. Furthermore, even a small dc offset in measured currents causes drift problems since a pure integration is used. The voltage model also becomes highly inaccurate at low speeds due to errors in the stator resistance estimate, as will be shown in Section 3.5.

Voltage Model Using Modified Integration

The drift problems of the pure integrator can be solved by modifying the integration procedure. The simplest modification is to replace the pure integrator with a low-pass filter (Takahashi and Noguchi, 1986), leading to

$$\frac{d\hat{\underline{\psi}}_R}{dt} = \hat{\underline{e}}_f - j\omega_k \hat{\underline{\psi}}_R - \alpha_v \hat{\underline{\psi}}_R \tag{3.6}$$

where α_v is the bandwidth of the low-pass filter. The flux estimate becomes erroneous even in steady state with accurate motor parameter estimates, and the estimator cannot be used at low speeds.

Shin et al. (2000) compensated the error due to the integrator replaced with a low-pass filter. They turned the angle and changed the magnitude of the output vector of the low-pass filter according to the calculated steady-state error. As shown in Publication I, the algorithm can be written in a simple form

$$\frac{d\hat{\underline{\psi}}_R}{dt} = \left[1 - j\lambda\,\mathrm{sign}(\hat{\omega}_s)\right]\hat{\underline{e}}_f - j\omega_k \hat{\underline{\psi}}_R - \lambda\,|\hat{\omega}_s|\,\hat{\underline{\psi}}_R \tag{3.7}$$

where λ is a gain related to the bandwidth of the low-pass filter. The estimator (3.7) can operate at lower frequencies than (3.6) due to the correct steady-state response. As shown by Ottersten and Harnefors (2002) using the linearized model, the system based on the

estimator (3.7) becomes unstable at low speeds. Harnefors et al. (2003) enhanced the estimator (3.7) according to

$$\frac{d\hat{\underline{\psi}}_R}{dt} = \left(\frac{\mu \,\mathrm{Re}\{\hat{\underline{e}}_f \hat{\underline{\psi}}_R^*\}}{\hat{\psi}_R^2} + j\frac{\mathrm{Im}\{\hat{\underline{e}}_f \hat{\underline{\psi}}_R^*\}}{\hat{\psi}_R^2} - j\lambda \,\mathrm{sign}(\hat{\omega}_s)\frac{\hat{\underline{e}}_f}{\hat{\underline{\psi}}_R} - j\omega_k - \lambda\,|\hat{\omega}_s| \right) \hat{\underline{\psi}}_R \tag{3.8}$$

by introducing an extra degree of freedom via the parameter μ. The steady-state response is still equal to that of the pure voltage model since $\mathrm{Re}\{\hat{\underline{e}}_f \hat{\underline{\psi}}_R^*\}$ is zero in steady state. By selecting $\mu = 1$, the estimator (3.8) reduces to (3.7). By suitably selecting μ, the damping of the system can be made better and the unstable region at low speeds can be reduced.

Holtz and Quan (2002) compensated the effect of the modified integration using the reference flux $\psi_{R,\mathrm{ref}}$ according to

$$\frac{d\hat{\underline{\psi}}_R}{dt} = \hat{\underline{e}}_f - j\omega_k \hat{\underline{\psi}}_R - \alpha_v \left(\hat{\underline{\psi}}_R - \underline{\psi}_{R,\mathrm{ref}} \right) \tag{3.9}$$

where $\underline{\psi}_{R,\mathrm{ref}} = \psi_{R,\mathrm{ref}} \exp[j(\hat{\vartheta}_s - \vartheta_k)]$ and ϑ_k is the angle of the reference frame. The original algorithm was written for stator flux estimation. Holtz and Quan (2003) recognized that a system using the estimator (3.9) has stability problems at low speeds when regenerating[2].

Other modifications of the integrator of the voltage model have been proposed by, for example, Bose and Patel (1997) and Hu and Wu (1998). Generally, these methods also suffer from stability problems at low speeds. Furthermore, the damping of the closed-loop system at higher speeds tends to be poor.

Voltage Model with Current-Model-Based Correction

The current model, which is the flux estimator based on (2.13) and (2.15), cannot be directly used in speed-sensorless drives since the rotor speed ω_m is required. The rotor speed in the current model can be replaced with its estimate $\hat{\omega}_m$, leading to speed-adaptive flux estimators discussed in Sections 3.3 and 3.4. Alternatively, the flux magnitude information (2.17) of the current model can be used in connection with the voltage model.

Based on (2.17), a steady-state estimate for the rotor flux magnitude can be written as $\hat{\psi}_{Rc} = \hat{L}_M i_{sd}$, where i_{sd} is the d component of the stator current in the estimated rotor flux reference frame. Ohtani et al. (1992) used this current-model-based estimate as

$$\frac{d\hat{\underline{\psi}}_R}{dt} = \hat{\underline{e}}_f - j\omega_k \hat{\underline{\psi}}_R - \alpha_v \left(\hat{\underline{\psi}}_R - \hat{\underline{\psi}}_{Rc} \right) \tag{3.10}$$

where $\hat{\underline{\psi}}_{Rc} = \hat{\psi}_{Rc} \exp[j(\hat{\vartheta}_s - \vartheta_k)]$. It can be shown that the linearized closed-loop system corresponding to the estimator (3.10) has an unstable region in the regenerating mode at low speeds.

Ambrožič et al. (1999) estimated the angular speed of the rotor flux by the voltage model and the magnitude of the rotor flux by the current model. The proposed estimator

[2]Fig. 20 in the paper by Holtz and Quan (2003) depicts the plugging-mode operation instead of the regenerating-mode operation according to the definitions used in this thesis (see Section 2.4).

written in the estimated rotor flux reference frame is

$$\frac{d\hat{\psi}_R}{dt} = -\frac{1}{\hat{\tau}_r}\hat{\psi}_R + \hat{R}_R i_{sd} \tag{3.11a}$$

$$\hat{\omega}_s = \frac{u_{sq} - \hat{R}_s i_{sq} - \hat{L}'_s \frac{d}{dt} i_{sq}}{\hat{\psi}_R + \hat{L}'_s i_{sd}} \tag{3.11b}$$

If another reference frame is preferred, (3.11) can be written in the general reference frame as

$$\frac{d\hat{\underline{\psi}}_R}{dt} = \left(-\frac{1}{\hat{\tau}_r} + \hat{R}_R \frac{\mathrm{Re}\{\underline{i}_s \hat{\underline{\psi}}_R^*\}}{\hat{\psi}_R^2} + j\frac{\mathrm{Im}\{\hat{\underline{e}}_f \hat{\underline{\psi}}_R^*\}}{\hat{\psi}_R^2} - j\omega_k \right) \hat{\underline{\psi}}_R \tag{3.12}$$

Ambrožič et al. recognized the regenerating-mode stability problems of the method. To stabilize the regenerating mode, they proposed to correct $\hat{\omega}_s$ using $\mathrm{Re}\{\hat{\underline{e}}_f \hat{\underline{\psi}}_R^*\}$, which should ideally be zero in steady state and which is not used in (3.12). However, Ambrožič et al. did not describe the correction mechanism.

Kim et al. (2003) corrected a voltage model estimator using a current-model-based estimate. Stator flux orientation control and the corresponding voltage and current models were used, but the proposed estimator loosely resembles the estimator (3.10). A suitable complex-valued gain (thus rotating the correction vector) is selected depending on the sign of the stator frequency and the sign of the estimated torque. Impressive but very noisy experimental results are shown in the paper, including operation at low speeds in the regenerating mode.

3.3 MRAS Flux Estimators

Generally, all speed-adaptive flux estimators can be seen as model-reference adaptive systems (MRAS). MRAS estimators consist of a reference model (which does not include the speed estimate $\hat{\omega}_m$) and an adjustable model (which includes the speed estimate). As shown in Fig. 3.2, the speed-adaptation law adjusts the speed estimate based on the outputs of the adjustable model and the reference model. This section deals with speed-adaptive estimators not falling into the group of full-order flux observers, which will be discussed in Section 3.4.

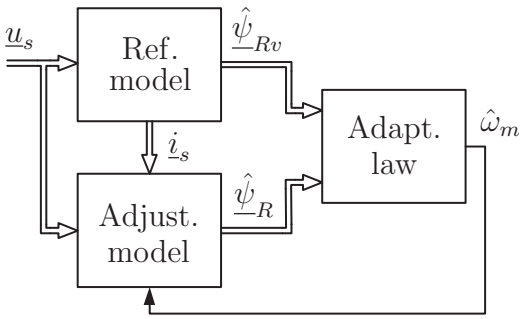

Figure 3.2. Example of MRAS flux estimator (Schauder, 1992). The reference model is the actual motor, while the adjustable model is the current model estimator (3.14). Assuming accurate parameter estimates, the pure voltage model (3.13) can be considered as part of the actual motor.

Voltage and Current Models

Schauder (1992) proposed a well-known MRAS estimator that is composed of the voltage model as a reference model and the current model as an adjustable model, i.e.,

$$\frac{d\hat{\underline{\psi}}_{Rv}}{dt} = \hat{\underline{e}}_f - j\omega_k \hat{\underline{\psi}}_{Rv} \tag{3.13}$$

$$\frac{d\hat{\underline{\psi}}_{R}}{dt} = -\left[\frac{1}{\hat{\tau}_r} + j(\omega_k - \hat{\omega}_m)\right]\hat{\underline{\psi}}_R + \hat{R}_R \underline{i}_s \tag{3.14}$$

where the voltage-model-based rotor flux estimate is marked by the subscript v. The rotor speed is estimated using the adaptation mechanism

$$\hat{\omega}_m = -\gamma_p\, \varepsilon - \gamma_i \int \varepsilon\, dt \tag{3.15}$$

where γ_p and γ_i are positive adaptation gains. The error term

$$\varepsilon = -\operatorname{Im}\left\{\hat{\underline{\psi}}_{Rv}\hat{\underline{\psi}}_R^*\right\} \tag{3.16}$$

is based on the component of the voltage-model-based rotor flux estimate $\hat{\underline{\psi}}_{Rv}$ that is perpendicular to the current-model-based estimate $\hat{\underline{\psi}}_R$. In the reference frame fixed to $\hat{\underline{\psi}}_R$, the error term reduces to $\varepsilon = -\hat{\psi}_{Rvq}\hat{\psi}_R$. Due to the integral action of (3.15), the error term is driven to zero in steady state.

The speed-adaptation law consisting of (3.15) and (3.16) was designed using the Popov hyperstability theory. The pure integration of (3.13) cannot be used in practice. Therefore, both the voltage model and the current model were augmented with first-order high-pass filters, and the corresponding auxiliary state variables were used in the error term (3.16). Unfortunately, the hyperstability conditions are not met after adding the high-pass filters. It was recognized by Schauder that adding the high-pass filters leads to instability at low speeds.

Actually, the instability due to the high-pass filters was already solved by Tamai et al. (1987) by taking the filters into account in the design of a speed-adaptation law. A high-pass filtered rotor flux

$$\underline{\psi}'_R = \frac{\frac{d}{dt} + j\omega_k}{\frac{d}{dt} + j\omega_k + \alpha}\,\underline{\psi}_R \tag{3.17}$$

was introduced, where α is the bandwidth of the filter. By estimating $\underline{\psi}'_R$ instead of $\underline{\psi}_R$, the pure integrator of the voltage model is avoided,

$$\frac{d\hat{\underline{\psi}}'_{Rv}}{dt} = \hat{\underline{e}}_f - j\omega_k \hat{\underline{\psi}}'_{Rv} - \alpha\hat{\underline{\psi}}'_{Rv} \tag{3.18}$$

where $\alpha = |\hat{\omega}_s|$ was selected by Tamai et al., $\hat{\omega}_s$ being the estimated angular frequency of the (non-filtered) rotor flux. The estimate of $\underline{\psi}'_R$ based on the current model becomes

$$\frac{d\hat{\underline{\psi}}'_{R}}{dt} = \hat{R}_R \underline{i}_s - \left(\frac{1}{\hat{\tau}_r} - j\hat{\omega}_m\right)\hat{\underline{\psi}}_R - j\omega_k\hat{\underline{\psi}}'_R - \alpha\hat{\underline{\psi}}'_R \tag{3.19}$$

where $\hat{\underline{\psi}}_R$ is the estimate of the non-filtered rotor flux obtained using (3.14). The speed-adaptation law designed using the Popov hyperstability theory is

$$\begin{aligned}\hat{\omega}_m = {} & \gamma_1 \operatorname{Im}\left\{\left(\hat{\underline{\psi}}'_{Rv} - \hat{\underline{\psi}}'_R\right)\hat{\underline{\psi}}^*_R\right\} \\ & + \frac{\gamma_1}{\hat{\tau}_r}\int \operatorname{Im}\left\{\left(\hat{\underline{\psi}}'_{Rv} - \hat{\underline{\psi}}'_R\right)\left(1 + j\hat{\tau}_r\hat{\omega}_r\right)\hat{\underline{\psi}}^*_R\right\} dt\end{aligned} \tag{3.20}$$

where γ_1 is a positive adaptation gain and $\hat{\omega}_r = \hat{\omega}_s - \hat{\omega}_m$ is the angular slip frequency estimate. Due to the factor $1 + j\hat{\tau}_r\hat{\omega}_r$ in the integral part of (3.20), the component of $\hat{\underline{\psi}}'_{Rv} - \hat{\underline{\psi}}'_R$ being parallel to $\hat{\underline{\psi}}_R$ is also used when $\hat{\omega}_r$ is nonzero. This change in the error projection stabilizes low speed operation if the parameter estimates are accurate. A different approach to stabilize the estimator is to use the speed-adaptation law consisting of (3.15) and (3.16), and to modify the filtering (3.17) as proposed by Nitayotan and Sangwongwanich (2001).

Reactive Power Models

Peng and Fukao (1994) proposed an MRAS estimator based on the variable

$$q_f = \frac{3}{2}\operatorname{Im}\left\{\underline{e}_f\underline{i}^*_s\right\} \tag{3.21}$$

whose magnitude represents the instantaneous reactive power (stator transient inductance L'_s excluded). Based on (2.14) and (2.15), two estimates for q_f can be written

$$\hat{q}_{fv} = \frac{3}{2}\operatorname{Im}\left\{\left(\underline{u}_s - \hat{L}'_s\frac{d\underline{i}_s}{dt} - j\omega_k\hat{L}'_s\underline{i}_s\right)\underline{i}^*_s\right\} \tag{3.22}$$

$$\hat{q}_f = \frac{3}{2}\operatorname{Im}\left\{\left(-\frac{1}{\hat{\tau}_r} + j\hat{\omega}_m\right)\hat{\underline{\psi}}_R\underline{i}^*_s\right\} \tag{3.23}$$

where the voltage-model-based estimate of q_f is marked by the subscript v and the rotor flux estimate $\hat{\underline{\psi}}_R$ is obtained using the current model (3.14). The error term to be used in the speed-adaptation mechanism (3.15) is

$$\varepsilon = \hat{q}_f - \hat{q}_{fv} \tag{3.24}$$

An advantage of the estimator is that it does not include the stator resistance estimate. However, according to Kubota et al. (1997), the estimator is unstable in the regenerating mode. Harnefors (2001) proposed an inherently sensorless flux estimator based on the instantaneous reactive power. Harnefors analyzed the stability using a linearized model and showed that the estimator becomes unstable in the regenerating mode.

3.4 Speed-Adaptive Full-Order Flux Observers

A speed-adaptive full-order flux observer was proposed by Kubota et al. (1993) and Yang and Chin (1993). The speed-adaptive full-order flux observer consists of a full-order flux observer augmented with a speed-adaptation loop as depicted in Fig. 3.3. The system can be considered as an MRAS: the actual motor behaves as a reference model and the observer, including the rotor speed estimate $\hat{\omega}_m$, as an adjustable model.

Observer Structure

Originally, the stator current estimate and the rotor flux estimate have been used as state variables, leading to

$$\frac{d\hat{\underline{\mathbf{z}}}}{dt} = \hat{\underline{\mathbf{F}}}\,\hat{\underline{\mathbf{z}}} + \hat{\mathbf{G}}\underline{u}_s + \underline{\mathbf{K}}\big(\underline{i}_s - \hat{\underline{i}}_s\big) \tag{3.25a}$$

$$\hat{\underline{i}}_s = \mathbf{H}\hat{\underline{\mathbf{z}}} \tag{3.25b}$$

which corresponds to (2.12). The observer state vector is $\hat{\underline{\mathbf{z}}} = [\,\hat{\underline{i}}_s \quad \hat{\underline{\psi}}_R]^T$ and estimates are marked by the symbol $\hat{}$. The matrix $\hat{\underline{\mathbf{F}}}$ and the observer gain $\underline{\mathbf{K}}$ are given by

$$\hat{\underline{\mathbf{F}}} = \begin{bmatrix} -\frac{1}{\hat{\tau}'_\sigma} - j\omega_k & \frac{1}{\hat{L}'_s}\left(\frac{1}{\hat{\tau}_r} - j\hat{\omega}_m\right) \\ \hat{R}_R & -\frac{1}{\hat{\tau}_r} - j\left(\omega_k - \hat{\omega}_m\right) \end{bmatrix}, \quad \underline{\mathbf{K}} = \begin{bmatrix} \underline{k}_s \\ \underline{k}_r \end{bmatrix} \tag{3.25c}$$

Choosing the stator and rotor flux estimates as state variables is preferred here. The modelling of magnetic saturation becomes simpler since no inductance derivatives are needed. In addition, the observer could be used with stator flux orientation control or direct torque control (Maes and Melkebeek, 2000) as well as with rotor flux orientation control. The full-order flux observer using the flux estimates as state variables corresponding to (2.11) is defined by

$$\frac{d\hat{\underline{\mathbf{x}}}}{dt} = \hat{\underline{\mathbf{A}}}\,\hat{\underline{\mathbf{x}}} + \mathbf{B}\underline{u}_s + \underline{\mathbf{L}}\big(\underline{i}_s - \hat{\underline{i}}_s\big) \tag{3.26a}$$

$$\hat{\underline{i}}_s = \hat{\mathbf{C}}\hat{\underline{\mathbf{x}}} \tag{3.26b}$$

where the observer state vector is $\hat{\underline{\mathbf{x}}} = [\hat{\underline{\psi}}_s \quad \hat{\underline{\psi}}_R]^T$, and the matrix $\hat{\underline{\mathbf{A}}}$ and the observer gain $\underline{\mathbf{L}}$ are given by

$$\hat{\underline{\mathbf{A}}} = \begin{bmatrix} -\frac{1}{\hat{\tau}'_s} - j\omega_k & \frac{1}{\hat{\tau}'_s} \\ \frac{1-\hat{\sigma}}{\hat{\tau}'_r} & -\frac{1}{\hat{\tau}'_r} - j\big(\omega_k - \hat{\omega}_m\big) \end{bmatrix}, \quad \underline{\mathbf{L}} = \begin{bmatrix} \underline{l}_s \\ \underline{l}_r \end{bmatrix} \tag{3.26c}$$

It can easily be shown that the transformation of the observer gains

$$\underline{\mathbf{L}} = \begin{bmatrix} \hat{L}'_s & 1 \\ 0 & 1 \end{bmatrix} \underline{\mathbf{K}} \tag{3.27}$$

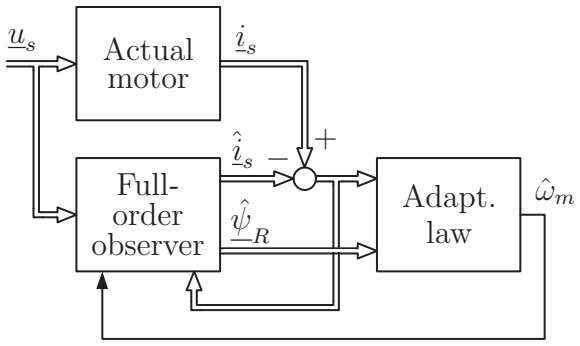

Figure 3.3. Example of speed-adaptive full-order flux observer (Kubota et al., 1993).

gives identical behaviour to observers (3.25) and (3.26). The transformation (3.27) is used to compare different observer gains found in the literature.

The rotor speed estimate is obtained using the adaptation mechanism (3.15). Different observer designs (i.e., selection of the observer gain $\underline{\mathbf{L}}$ and the error term ε of the speed-adaptation law) lead to different behaviour of the observer. In the following, observer designs proposed in the literature are described.

Conventional Observer Design

Kubota et al. (1993) and Yang and Chin (1993) used

$$\varepsilon = \mathrm{Im}\left\{\left(\underline{i}_s - \hat{\underline{i}}_s\right)\hat{\underline{\psi}}_R^*\right\} \tag{3.28}$$

as the error term of the speed-adaptation law in their original design. The speed-adaptation law is based on the component of the current estimation error that is perpendicular to $\hat{\underline{\psi}}_R$. The error term reduces to $\varepsilon = (i_{sq} - \hat{i}_{sq})\hat{\psi}_R$ in the reference frame of the estimated rotor flux. Kubota et al. derived the adaptation law using the Lyapunov stability theory, whereas Yang and Chin used the Popov hyperstability theory. However, the stability of the adaptation law is not guaranteed. In their derivation, Kubota et al. neglected a term including the actual rotor flux (which is not measurable) as shown by Tajima et al. (2002). Suwankawin and Sangwongwanich (2002) showed that the positive-realness condition is not satisfied in the derivation by Yang and Chin.

Kubota et al. (1993) and Yang and Chin (1993) proposed the observer gain

$$\underline{\mathbf{L}} = (k_1 - 1)\,\hat{R}_s \begin{bmatrix} k_1 + 1 \\ k_1 - \frac{\hat{\tau}_s'}{\hat{\tau}_r'} + j\hat{\tau}_s'\hat{\omega}_m \end{bmatrix} \tag{3.29}$$

where k_1 is a positive parameter. Assuming constant rotor speed estimate (i.e., with the dynamics of the speed-adaptation loop ignored), the observer gain (3.29) places the observer poles in the stator reference frame in proportion to the motor poles. Kubota et al. selected $k_1 = 1$ leading to $\underline{\mathbf{L}} = [0 \quad 0]^T$ whereas Yang and Chin used $k_1 = 1.2$.

It is well known that induction motor drives using the conventional observer design become unstable when regenerating at low speeds (e.g., Suwankawin and Sangwongwanich, 2002). Furthermore, a poorly damped region appears at higher speeds as shown in Publication V. Evidently, the speed-adaptation loop should not be ignored when considering the observer dynamics.

Voltage and Current Models

As shown in Publication V, the estimator by Schauder (1992) described in Section 3.3 is a special case of the speed-adaptive full-order flux observer. By choosing the observer gain

$$\underline{\mathbf{L}} = \begin{bmatrix} -\hat{R}_s \\ \hat{R}_R \end{bmatrix} \tag{3.30}$$

the voltage model for the stator flux estimate and the current model for the rotor flux estimate are obtained from (3.26). The error term (3.28) of the speed-adaptation law can be written as

$$\varepsilon = -\frac{1}{\hat{L}_s'}\,\mathrm{Im}\left\{\left(\hat{\underline{\psi}}_s - \hat{L}_s'\underline{i}_s\right)\hat{\underline{\psi}}_R^*\right\} \tag{3.31}$$

based on (3.26b). Comparison of (3.31) and (3.16) shows that the error terms are identical; only the adaptation gains need to be scaled. The factor $\hat{\underline{\psi}}_s - \hat{L}'_s \underline{i}_s$ equals the output $\hat{\underline{\psi}}_{Rv}$ of the voltage model (3.13) whereas $\hat{\underline{\psi}}_R$ equals the output of the current model (3.14).

Modified Observer Gain — Conventional Speed-Adaptation Law

Kubota et al. (2002) realized the regenerating-mode stability problems in their original design (Kubota et al., 1993). Based on the linearized model of the system, they redesigned the observer gain (3.29) by introducing a parameter

$$k_1 = \begin{cases} \frac{1}{2}\frac{\hat{\omega}_s}{\hat{\omega}_m}\left(1 + \frac{\hat{\tau}'_s}{\hat{\tau}'_r}\right), & \text{if } \hat{\omega}_s\hat{\omega}_r < 0 \\ 1, & \text{otherwise} \end{cases} \tag{3.32}$$

It can be shown using the linearized model that the observer design stabilizes the regenerating mode at low speeds. The behaviour in the motoring mode is equal to the original observer design.

The flux observer by Tsuji et al. (2001) can be considered as a speed-adaptive full-order flux observer having the observer gain

$$\underline{\mathbf{L}} = \begin{bmatrix} -\hat{R}_s + k_2\hat{L}'_s \\ \hat{R}_R \end{bmatrix} \tag{3.33}$$

The gain selection corresponds to the voltage model corrected with the current estimation error due to the parameter k_2 and the current model, see also (3.30). To reduce the unstable region in the regenerating mode, Tsuji et al. selected the parameter k_2 ten times smaller in the regenerating mode than in the motoring mode.[3] It can be shown that the speed-adaptation law used by Tsuji et al. corresponds to the conventional speed-adaptation law.

Suwankawin and Sangwongwanich (2003) proposed the observer gain

$$\underline{\mathbf{L}} = \begin{bmatrix} -\hat{R}_s + k_3\hat{L}'_s\left(\frac{1}{\hat{\tau}_r} + j\hat{\omega}_m\right) \\ \hat{R}_R \end{bmatrix} \tag{3.34}$$

where k_3 is a positive parameter. It can be shown using the linearized model that the observer design results in a stable system but the damping at higher speeds is poor.

Zero Observer Gain — Modified Speed-Adaptation Law

Hofmann and Sanders (1998) proposed the error term

$$\varepsilon = \mathrm{Im}\left\{\left(\underline{i}_s - \hat{\underline{i}}_{sc}\right)\left(\hat{\underline{i}}_s - \hat{\underline{i}}_{sc}\right)^*\right\} \tag{3.35a}$$

where

$$\hat{\underline{i}}_{sc} = \frac{\hat{R}_s - j\hat{\omega}_s\left(\frac{\hat{L}_M}{2} + \hat{L}'_s\right)}{\hat{R}_s^2 + (\hat{L}_M + \hat{L}'_s)\hat{L}'_s\hat{\omega}_s^2}\underline{u}_s \tag{3.35b}$$

is the estimated centre point of the current locus when the slip frequency (or the rotor speed) is varied. Therefore, the sign of the angle between vectors $\underline{i}_s - \hat{\underline{i}}_{sc}$ and $\hat{\underline{i}}_s - \hat{\underline{i}}_{sc}$

[3] Tsuji et al. used the current references in the rotor dynamics of the observer (instead of the measured currents) and they also assumed constant $i_{sd,\mathrm{ref}}$. The parameter k_2 was denoted by $1/T_c$ in the paper.

depends on the sign of the speed estimation error under the assumption of electrical steady state.

Hoffmann and Koch (1998) designed the speed-adaptation law assuming the current estimation error in steady state.[4] The proposed error term can be written as

$$\varepsilon = \mathrm{Im}\left\{ \left(\underline{i}_s - \hat{\underline{i}}_s\right) \hat{\underline{\psi}}_R^* e^{-j\phi} \right\} \tag{3.36}$$

where the factor $\exp(-j\phi)$ changes the direction of the error projection. Hoffmann and Koch selected the factor as $\exp(-j\phi) = (1 + j\hat{\omega}_r\hat{\tau}_r)/\sqrt{1 + \hat{\omega}_r^2\hat{\tau}_r^2}$, corresponding to the angle

$$\phi = -\arctan(\hat{\omega}_r\hat{\tau}_r) \tag{3.37}$$

which guarantees the correct sign of the error term under the steady-state assumption. Using a linearized model, it can be shown that the observer design stabilizes the regenerating mode at low speeds. However, there is an unstable region in the motoring mode at low speeds (which could be stabilized by, for example, setting $\phi = 0$ in the motoring mode). It is worth noting that, based on (2.17) and (2.18), $\omega_r\tau_r = i_{sq}/i_{sd}$ holds in steady state in the rotor flux reference frame.

To stabilize the regeneration mode operation, Tajima et al. (2002) proposed to augment the conventional error term according to

$$\varepsilon = (i_{sq} - \hat{i}_{sq})\hat{\psi}_R - \gamma_2 \,\mathrm{sign}(\hat{\omega}_s)\left(i_{sd} - \hat{i}_{sd}\right)|\hat{i}_{sq}| \tag{3.38}$$

where γ_2 is a positive gain and the estimated rotor flux reference frame is assumed. Tajima et al. mentioned that γ_2 should be adjusted according to the load level. Furthermore, $\gamma_p = 0$ was used in the adaptation mechanism (3.15). The error term was partly formed on the basis of simulation analysis, and no stability analysis was given. Assuming $\hat{i}_{sq} = \hat{\omega}_r\hat{\psi}_R/\hat{R}_R$, the error term (3.38) can be expressed in a general reference frame as

$$\varepsilon = \mathrm{Im}\left\{ \left(\underline{i}_s - \hat{\underline{i}}_s\right) \hat{\underline{\psi}}_R^* \left(1 - j\gamma_2 \,\mathrm{sign}(\hat{\omega}_s)\frac{|\hat{\omega}_r|}{\hat{R}_R}\right) \right\} \tag{3.39}$$

Comparison of (3.37) and (3.39) reveals that the error projection is changed to the same direction only in the regenerating mode.

Rashed et al. (2003b) proposed the error term

$$\varepsilon = \mathrm{Im}\left\{ \left(\underline{i}_s - \hat{\underline{i}}_s\right) \hat{\underline{\psi}}_R^* (1 - j\gamma_3) \right\} \tag{3.40a}$$

where

$$\gamma_3 = \begin{cases} \hat{\tau}_r\hat{\omega}_m, & \text{if } \hat{\tau}_r|\hat{\omega}_m| < L \\ \mathrm{sign}(\hat{\omega}_m)L, & \text{otherwise} \end{cases} \tag{3.40b}$$

The limit value L was selected as

$$L = \begin{cases} 2\hat{\tau}_r|\hat{\omega}_r|, & \text{if } \hat{\omega}_s\hat{\omega}_r < 0 \\ \min\left\{ \frac{1}{2\hat{\tau}_r'|\hat{\omega}_r|},\, 2\hat{\tau}_r|\hat{\omega}_r| \right\}, & \text{otherwise} \end{cases} \tag{3.40c}$$

The error term was designed using the linearized model of the observer, and, according to the analysis, the speed-adaptation law stabilizes the system at low speeds. It was also stated by Rashed et al. that the selection (3.40) is an example of stable design and that there are other stabilizing choices of γ_3. The behaviour at higher speeds was not considered in the paper.

[4] The observer structure was not described in the paper, but it seems to be the full-order flux observer with $\underline{\mathbf{L}} = [0 \quad 0]^T$.

Modified Observer Gain — Modified Speed-Adaptation Law

Harnefors and Nee (1997) designed an observer gain by ignoring the dynamics of the speed-adaptation loop and using a pole placement. The poles were placed so that properties close to the current and voltage models are obtained at low and high speeds, respectively, and that good damping and convergence are achieved. The observer gain was

$$\underline{\mathbf{L}} = \begin{bmatrix} -\hat{R}_s + \hat{L}'_s \left\{ |\hat{\omega}_s| + \alpha + f\alpha \left[-1 + j \operatorname{sign}(\hat{\omega}_s) \right] \right\} \\ \hat{R}_R + f\hat{L}'_s \alpha \left[-1 + j \operatorname{sign}(\hat{\omega}_s) \right] \end{bmatrix} \tag{3.41a}$$

where

$$f = \begin{cases} \frac{|\hat{\omega}_s|}{\omega_\Delta}, & \text{if } |\hat{\omega}_s| < \omega_\Delta \\ 1, & \text{if } |\hat{\omega}_s| \geq \omega_\Delta \end{cases} \tag{3.41b}$$

The parameter α was selected according to the bandwidth of the current controller and ω_Δ is the desired transition frequency between the approximative current and voltage models. It can be shown that the damping of the speed-adaptive observer using (3.41) with properly selected α is comparatively good at higher speeds. Based on a simplified recursive least squares estimation, Harnefors and Nee also proposed the error term

$$\varepsilon = \operatorname{Im} \left\{ \left(\underline{i}_s - \hat{\underline{i}}_s \right) \underline{\hat{\psi}}^*_R \left[1 - j \operatorname{sign}(\hat{\omega}_s) \right] \right\} \tag{3.42}$$

The speed-adaptation gains were $\gamma_p = 0$ and $\gamma_i = 0.1 f \alpha^2 \hat{L}'_s / \hat{\psi}^2_R$, where f and α correspond to those used in the observer gain. It can be shown that the speed-adaptation law (3.42) reduces the unstable region in the regenerating mode but causes stability problems in the motoring mode.

Maes and Melkebeek (2000) proposed an observer gain shifting the observer poles to the left in the complex plane compared to the motor poles. The dynamics of the speed-adaptation loop were ignored in the design. Furthermore, the speed-adaptation law

$$\varepsilon = \operatorname{Im} \left\{ \left(\underline{i}_s - \hat{\underline{i}}_s \right) \underline{\hat{\psi}}^*_s \right\} \tag{3.43}$$

based on the current estimation error perpendicular to the estimated stator flux was proposed. However, the stability of the adaptation law is not guaranteed as shown in Publication VI, and stability problems still exist in the regenerating mode. Peterson (1996) proposed a speed-adaptation law similar to (3.43). Peterson measured the stator voltage and implemented the calculation of the stator dynamics using analogue integrators.

Hasegawa and Matsui (2002) modified the error term of the speed-adaptation law according to (3.36). Under the assumption of the current estimation error being in steady state and the angular stator frequency equalling the angular rotor speed, the angle ϕ was selected so that the vectors $(\underline{i}_s - \hat{\underline{i}}_s) \exp(-j\phi)$ and $\underline{\hat{\psi}}_R$ are perpendicular. The approach is not general: it can be shown that unstable regions are encountered with, for example, the observer gain $\underline{\mathbf{L}} = [0 \quad 0]^T$ both in the motoring and regenerating modes. Hasegawa and Matsui designed the observer gain using an H_∞ approach. Since the proposed observer gain requires heavy calculation [minimization of parameters constrained by linear matrix inequalities (LMI)], the method may be impractical. However, the proposed observer design may stabilize the system.

In Publication V, the simple observer gain

$$\underline{\mathbf{L}} = \lambda \begin{bmatrix} 1 + j \operatorname{sign}(\hat{\omega}_m) \\ -1 + j \operatorname{sign}(\hat{\omega}_m) \end{bmatrix} \tag{3.44a}$$

where

$$\lambda = \begin{cases} \lambda' \frac{|\hat{\omega}_m|}{\omega_\lambda}, & \text{if } |\hat{\omega}_m| < \omega_\lambda \\ \lambda', & \text{if } |\hat{\omega}_m| \geq \omega_\lambda \end{cases} \tag{3.44b}$$

giving well-damped dynamics up to very high speeds was proposed. Parameters λ' and ω_λ are positive constants. The observer gain (3.44) is basically constant at higher speeds. Furthermore, a method to vary the speed-adaptation gains γ_p and γ_i in the field-weakening region was proposed in Publication V. The observer gain is designed especially for nominal and high-speed operation whereas the problems at low speeds are handled by modifying the error term of the speed-adaptation law according to (3.36) as described in Publication VI. The angle ϕ stabilizing the regenerating mode is selected as

$$\phi = \begin{cases} \phi_{\max} \operatorname{sign}(\hat{\omega}_s) \left(1 - \frac{|\hat{\omega}_s|}{\omega_\phi}\right), & \text{if } |\hat{\omega}_s| < \omega_\phi \text{ and } \hat{\omega}_s \hat{\omega}_r < 0 \\ 0, & \text{otherwise} \end{cases} \tag{3.45}$$

where $\phi_{\max}$ and ω_ϕ are positive constants. The steady-state relation given in Publication VI can be applied in choosing $\phi_{\max}$ and ω_ϕ. An advantage of (3.45) is that only the information of $\operatorname{sign}(\hat{\omega}_s)$ and $\operatorname{sign}(\hat{\omega}_s \hat{\omega}_r)$ is crucial whereas the observer gain using (3.32), for example, is a function of $\hat{\omega}_s$ and $\hat{\omega}_r$.

3.5 Effect of Parameter Errors

Actual parameters of the motor vary with temperature (resistances) and magnetic saturation (inductances). A model of magnetic saturation can be used, but the changes in temperature are much more difficult to handle. The effect of parameter errors on the accuracy of the flux estimator is crucial since it determines the robustness of the overall system. As described in Publications IV and VI, the effect of parameter errors can be studied by means of a steady-state expression for $\underline{\hat{\psi}}_R / \underline{\psi}_R$. Steady-state expressions are obtained by substituting $d/dt = 0$ and $\omega_k = \omega_s$, where ω_s is the angular stator frequency (being equal to the angular frequencies of the estimated and actual rotor fluxes in steady state). The effects of parameter errors on four speed-adaptive full-order flux observer designs have been compared in Publication VI. As a reference, the effects of parameter errors on two inherently sensorless flux estimators are evaluated in the following. The parameters of a 2.2-kW motor described in Chapter 4 are used.

Voltage Model and Modified Integrators

Using (2.9), (2.10), and (3.3), the steady-state expression for $\underline{\hat{\psi}}_R / \underline{\psi}_R$ corresponding to the voltage model can be derived (Jansen and Lorenz, 1994), the result being

$$\frac{\underline{\hat{\psi}}_R}{\underline{\psi}_R} = 1 + \frac{1 + j\omega_r \tau_r}{L_M} \left(L'_s - \hat{L}'_s - j \frac{R_s - \hat{R}_s}{\omega_s} \right) \tag{3.46}$$

The solid curves in Fig. 3.4 illustrate the expression for $\underline{\hat{\psi}}_R / \underline{\psi}_R$ obtained using (3.46) at low stator frequencies when erroneous parameter estimates are used. The curves in Fig. 3.4(a,b) correspond to no-load operation, and the curves in Fig. 3.4(c,d,e,f) correspond approximately to the rated-load operation, i.e., the angular slip frequency ω_r is equal to

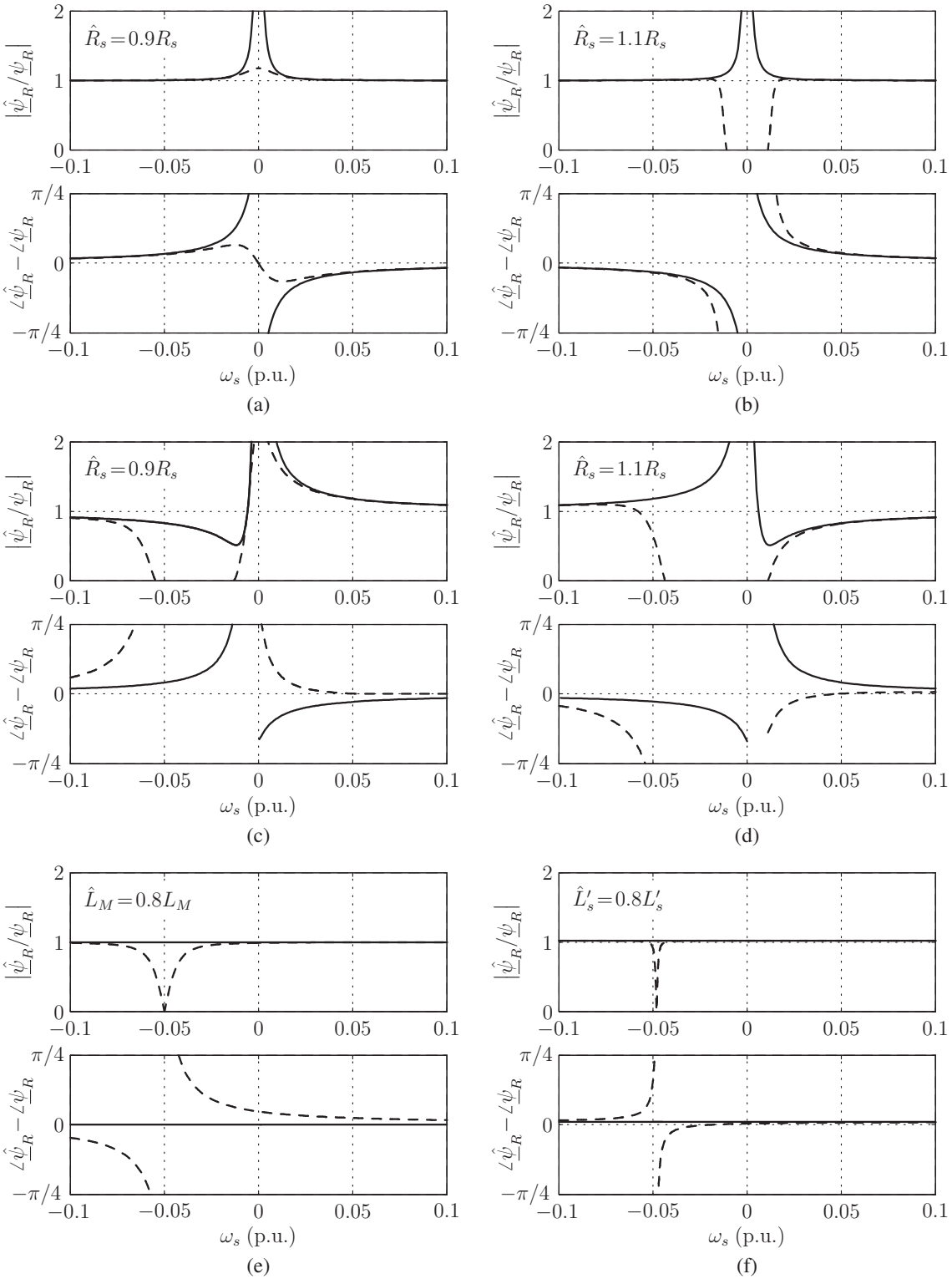

Figure 3.4. Effect of parameter errors on $\hat{\underline{\psi}}_R/\underline{\psi}_R$: (a,b) actual slip frequency is $\omega_r = 0$; (c,d,e,f) $\omega_r = \omega_{rN} = 0.05$ p.u. The solid line corresponds to the voltage model (and modified integrators); the dashed line corresponds to the estimator (3.10), where $\alpha_v = 1/\hat{\tau}_r$ is used. Erroneous parameter estimates are given in subfigures.

the rated slip ω_{rN}. All three operating modes of induction motors can be seen in Fig. 3.4(c,d,e,f).

Small errors in the stator resistance estimate $\hat{R}_s$ make it impossible to operate at low speeds, even without load. The effect of errors in the stator transient inductance $\hat{L}'_s$ are almost negligible. The rotor resistance estimate $\hat{R}_R$ and the magnetizing inductance estimate $\hat{L}_M$ are not involved in the voltage model. However, $\hat{R}_R$ has an effect on the accuracy of the rotor speed estimate as can be seen from (3.4).

The expression for $\underline{\hat{\psi}}_R/\underline{\psi}_R$ corresponding to the voltage-model-based estimators (3.7) and (3.8) using modified integration is equal to (3.46). Therefore, problems at low speeds are expected even in no-load operation. Since $\psi_{R,\mathrm{ref}}$ is included in the estimator (3.9), the expression for $\underline{\hat{\psi}}_R/\underline{\psi}_R$ depends on how the flux is controlled. Based on measurements, Holtz and Quan used a flux controller having an integral effect, leading to $\underline{\psi}_{R,\mathrm{ref}} = \underline{\hat{\psi}}_R$ in steady state. Consequently, the expression for $\underline{\hat{\psi}}_R/\underline{\psi}_R$ corresponding to (3.9) is also equal to (3.46).

Voltage Model with Current-Model-Based Correction

When the estimator (3.10) is used, the expression

$$\frac{\underline{\hat{\psi}}_R}{\underline{\psi}_R} = \frac{j\omega_s + \left[R_s - \hat{R}_s + j\omega_s\big(L'_s - \hat{L}'_s\big)\right]\frac{1+j\omega_r\tau_r}{L_M} + \alpha_v\frac{\underline{\hat{\psi}}_{Rc}}{\underline{\psi}_R}}{\alpha_v + j\omega_s} \tag{3.47a}$$

holds in steady state, where $\underline{\hat{\psi}}_{Rc}$ can be written as

$$\begin{aligned}\underline{\hat{\psi}}_{Rc} &= \hat{L}_M\frac{\mathrm{Re}\big\{\underline{i}_s\underline{\hat{\psi}}^*_R\big\}}{\hat{\psi}^2_R}\underline{\hat{\psi}}_R \\ &= \frac{\hat{L}_M}{L_M}\left(\frac{\mathrm{Re}\big\{\underline{\psi}_R\underline{\hat{\psi}}^*_R\big\}}{\hat{\psi}^2_R} - \omega_r\tau_r\frac{\mathrm{Im}\big\{\underline{\psi}_R\underline{\hat{\psi}}^*_R\big\}}{\hat{\psi}^2_R}\right)\underline{\hat{\psi}}_R\end{aligned} \tag{3.47b}$$

To obtain the latter form of (3.47b), the steady-state expression

$$\underline{i}_s = \frac{1 + j\tau_r\omega_r}{L_M}\underline{\psi}_R \tag{3.48}$$

based on (2.13) and (2.15) was used. The dashed curves in Fig. 3.4 illustrate the expression for $\underline{\hat{\psi}}_R/\underline{\psi}_R$ which is solved from (3.47) using iteration. Only the solutions that are continuous with the rated-speed solution fulfilling the condition $\underline{\hat{\psi}}_R/\underline{\psi}_R \approx 1$ are shown. A similar approach is used in Publication VI.

The existence of a steady-state solution of $\underline{\hat{\psi}}_R/\underline{\psi}_R$ does not guarantee that the solution is stable. On the other hand, absence, discontinuity, or significant inaccuracy of a steady-state solution is a clear indicator of stability problems in that operating point. According to simulations and experiments, fast transients through the unstable region are usually possible.

It can be seen that the accuracy of the estimator (3.10) in no-load operation with an underestimated stator resistance in Fig. 3.4(a) is much better than the accuracy of the voltage model. According to Fig. 3.4(b), an overestimated stator resistance may cause problems in no-load operation. Actually, there is a solution fulfilling the condition $\underline{\hat{\psi}}_R/\underline{\psi}_R \approx 1$ at very

low speeds, but that solution is discontinuous with the desirable rated-speed solution and, therefore, not shown in Fig. 3.4(b). The accuracy of the estimator (3.10) in the rated-load operation in Fig. 3.4(c,d) is slightly better in the motoring and plugging modes than the accuracy of the voltage model. Consequently, no-load and rated-load zero-speed operation can be achieved in practice when using the estimator (3.10). On the other hand, the accuracy of the estimator (3.10) in the regenerating mode at low speeds is much worse than the accuracy of the voltage model based on Fig. 3.4(c,d,e,f). The regenerating-mode operation could probably be enhanced using similar methods as discussed by Ambrožič et al. (1999) or proposed by Kim et al. (2003), see p. 22.

It is interesting that the effects of parameter errors on the estimator (3.10) and on some speed-adaptive observer designs are very similar. This can be seen by comparing Fig. 3.4 to the results in Publication VI. Furthermore, it can be seen that the observer design proposed in Publication VI is generally better than the voltage model or the estimator (3.10) when parameter errors exist.

3.6 On-Line Stator Resistance Estimation

To handle the stator resistance variations, on-line stator resistance estimators have been proposed in the literature. In connection with voltage-model-based flux estimators, the stator resistance estimators are typically based on the fact that the flux-emf is perpendicular to the rotor flux in steady state:[5]

$$\mathrm{Re}\{\underline{e}_f \underline{\psi}_R^*\} = 0 \tag{3.49}$$

The estimators by Mitronikas et al. (2001) and Holtz and Quan (2003) were derived using the current-model-based flux-emf (2.15) in the condition (3.49), which then reduces to $\psi_R = L_M i_{sd}$ in the rotor flux reference frame[6]. Essentially the same information is used as a correction signal in some flux estimators, for example, in the estimator (3.10).

Ambrožič et al. (1999) used the voltage-model-based flux-emf (2.14) and the condition (3.49) for the stator resistance estimation. The stator resistance was estimated only in the motoring mode since the same information was used in the flux estimator for stabilizing the regenerating mode. In connection with speed-adaptive full-order flux observers, the stator resistance is often estimated using the term $\mathrm{Re}\{(\underline{i}_s - \hat{\underline{i}}_s)\hat{\underline{i}}_s^*\}$, which should ideally be zero in steady state (e.g., Kubota et al., 1993).

Most of the stator resistance estimators proposed in the literature are derived under simplifying assumptions (such as $\hat{\omega}_m = \omega_m$) and the stability analysis of the system is not carried out. It is not sufficient that the speed estimation and the stator resistance estimation are individually stable since the interaction between the two estimators may destabilize the overall system (Rashed et al., 2003a). The system including simultaneous estimation of the speed and the stator resistance should be considered as a multiple-input multiple-output (MIMO) system, as was the case in the design proposed by Rashed et al.

In this work, stator resistance estimators are not studied. In practice, stator voltage measurement or a very accurate model of the inverter nonlinearities (using a voltage-feedback based dead-time compensation) may be necessary if a stator resistance estimator is used.

[5] Using the rotor current, the fact can be written as $\mathrm{Re}\{\underline{i}_R \underline{\psi}_R^*\} = 0$.

[6] The equal condition appears more complicated in the stator flux reference frame used by Mitronikas et al. and Holtz and Quan.

3.7 Flux Estimators Combined with Signal Injection

The dynamic response of signal-injection methods (see Chapter 1) is typically only moderate or they suffer from torque ripples due to unmodelled dynamics. To circumvent these problems, Ide et al. (2002) combined a signal-injection method with the speed-adaptive observer using the observer gain $\underline{\mathbf{L}} = [0 \quad 0]^T$. The error term

$$\varepsilon = \mathrm{HPF}\left\{\mathrm{Im}\left\{\left(\underline{i}_s - \hat{\underline{i}}_s\right)\hat{\underline{\psi}}_R^*\right\}\right\} + \mathrm{LPF}\left\{\gamma_\vartheta f_\vartheta\right\} \tag{3.50}$$

of the speed-adaptation law was used, where HPF denotes high-pass filtering, γ_ϑ is a gain, and f_ϑ is the error signal obtained using a high-frequency signal-injection method by Ha and Sul (1999). Due to the filters in (3.50), the conventional error term is active at transients, whereas the signal-injection term dominates in steady state. The filters are designed so that both the conventional error term and the signal-injection term are in use at low speeds, whereas only the conventional error term is used at higher speeds. Due to the integral action of the adaptation mechanism (3.15) and the high-pass filter in (3.50), the signal f_ϑ is driven to zero in steady state at low speeds.

A method combining advantages of the low-frequency signal-injection approach by Leppänen and Luomi (2002) and the speed-adaptive full-order flux observer is proposed in Publication VII. A low-frequency (25 Hz for a 2.2-kW motor) alternating current is superimposed on the flux-producing component of the stator current in the estimated rotor flux reference frame. The response of the mechanical system is used to calculate the error signal f_ϑ (having the same sign as the error angle of the rotor flux estimate) which is used in the error term resembling (3.50). The high-pass-filter in (3.50) is modified to ensure proper transient operation. The observer gain (3.44) is used, resulting in a wide speed range from zero to very high speeds. Experimental results are shown in Publication VII, including very slow speed reversals and long-term zero-frequency operation under rated load torque, as well as fast speed and load torque transients.

To ensure the observability of the flux and the speed in the vicinity of the zero stator frequency, Rashed et al. (2003b) superimposed a low-frequency (15 Hz) alternating current on the torque-producing component of the stator current. The speed-adaptive full-order flux observer using the observer gain $\underline{\mathbf{L}} = [0 \quad 0]^T$ and the speed-adaptation law corresponding to (3.40) was used. A drawback of the method is that high torque and speed ripples are caused.

Chapter 4

Experimental Setup

The experimental setup depicted in Fig. 4.1 was used to investigate the methods in the Publications. Technical data of the laboratory hardware is given in Table 4.1. The induction motor (IM) is used for the investigation of control methods, and the permanent magnet (PM) servo motor is used as the loading machine. The induction motor is a general-purpose three-phase squirrel-cage induction motor. The parameters of the induction motor are given in Table 4.2. Both motors are fed by frequency converters (Danfoss VLT5004 and ABB Bivector), which are connected to the 400-V 50-Hz three-phase supply.

Control algorithms for the induction motor are executed in a dSpace DS1103 PPC controller board plugged in a host PC. Six PWM gate signals of the VLT5004 converter are generated directly by the DS1103 controller board. This is possible due to the replacement of the original controller board of the VLT5004 converter with an interface and protection board designed for use with the DS1103 board. The interface and protection board and the required signal conditioning have been designed and manufactured at Aalborg University (Teodorescu et al., 2000).

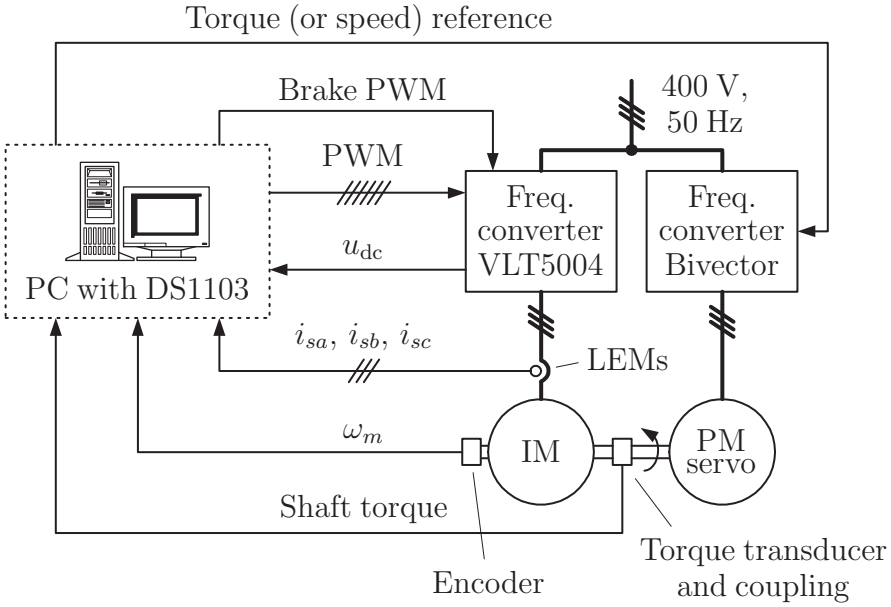

Figure 4.1. Experimental setup. Control of induction motor (IM) is investigated, and permanent magnet (PM) servo motor is used as loading machine. Measured shaft torque and rotor speed are used only for monitoring of speed-sensorless methods.

Table 4.1. Technical data of laboratory hardware. Current and voltage values are rms values. Three-phase voltages are phase-to-phase voltages.

Induction motor	ABB M2AA 100LA 3GAA102001-ADA
Rating plate	380…420 V, 50 Hz, 1 430 r/min, 2.2 kW, 5.0 A, $\cos\varphi = 0.81$
Moment of inertia	0.0069 kgm^2
Freq. converter for IM	Danfoss VLT5004 P T5 B20 EB R3 (modified)
Supply voltage	380…500 V (50/60 Hz)
Output voltage	0…100 % of supply voltage
Max. const. output current	5.6 A
Output frequency	0…1 000 Hz
PM servo motor	ABB 8C5 230 00YA02SL3MB
Rating plate	315 V, 3 000 r/min, cont. stall torque 21.5 Nm (14.1 A), peak stall torque 75.3 Nm (54.6 A)
Moment of inertia	0.0040 kgm^2
Freq. converter for PM servo	ABB Bivector 535 “25”
Rated supply voltage	400 V (50/60 Hz)
Rated output voltage	400 V
Rated cont. output current	25.0 A
Current transducers	LEM LA 55-P/SP1
Bandwidth	0…200 kHz (-1 dB)
Accuracy (at 25°C, rated current)	$\pm$0.9 %
Incremental encoder	Leine & Linde 186 90311
Line counts	2 048 ppr
Moment of inertia	$42 \cdot 10^{-6}$ kgm^2
Torque transducer	HBM K-T10F-050Q-SU2-G-1-W1-Y
Rated torque	50 Nm
Maximum speed	15 000 r/min
Torsional stiffness	160 kNm/rad
Bandwidth	0…1 kHz (-3 dB)
Moment of inertia	0.0017 kgm^2
Coupling	HBM BSD-MODULFLEX for K-T10F
Torsional stiffness	24 kNm/rad
Moment of inertia (incl. joint)	0.0029 kgm^2
Controller board	dSpace DS1103 PPC
Master processor	PowerPC 604e (400 MHz, 2 MB local SRAM, 128 MB global DRAM)
Slave processor	Texas Instruments TMS320F240 DSP (20 MHz, 3-phase PWM generation)

In speed-sensorless methods, three phase currents and the dc-link voltage u_{dc} of the VLT5004 converter are used as feedback signals for the controller. The phase currents are measured using external LEM current transducers. The dc-link voltage is measured using the original internal sensor circuitry of the VLT5004 converter. The measured shaft torque and the rotor speed ω_m are available for monitoring purposes. Furthermore, the DS1103 board is used to adjust the load profile of the servo drive and to control the brake chopper of the VLT5004 converter. Four-quadrant operation is possible since both frequency converters are equipped with brake resistors.

Table 4.2. Parameters of 2.2-kW 4-pole 400-V 50-Hz induction motor and load.

Stator resistance R_s	3.67 Ω
Rotor resistance R_R	2.10 Ω
Magnetizing inductance L_M	0.224 H
Stator transient inductance L'_s	0.0209 H
Rated speed	1 430 r/min
Rated current	5.0 A
Rated torque	14.6 Nm
Rated power factor $\cos\varphi$	0.81
Total moment of inertia	0.0155 kgm^2
Viscous friction coefficient	0.0025 Nm·s

The DS1103 board includes a PowerPC 604e RISC processor and a Texas Instruments TMS320F240 DSP, acting as the master and slave processors, respectively. The built-in modulator of the slave processor is used to generate three-phase PWM gate signals, whereas the control algorithms are executed in the master processor. The PWM interrupt of the slave processor is used to synchronize the master processor (and the sampling) to the modulation. In the experiments, both the switching frequency and the sampling frequency were 5 kHz. A software-based current feedforward compensation is applied for dead times and power device voltage drops (Pedersen et al., 1993).

The control algorithms were programmed in the MATLAB/Simulink environment, using mainly S-function blocks written using the C language. Since the resulting algorithms are discrete, the Simulink models are also implemented as discrete models. After graphically connecting all Simulink blocks, the Simulink Real-Time Workshop is used to generate the C code from the Simulink Model. Then, the dSpace Real-Time Interface is used to build, download, and execute the code on the DS1103 board.

Chapter 5

Summary of Publications

The abstracts of the Publications are reprinted in Section 5.1. Publication I deals with a voltage-model-based flux estimator whereas the other Publications deal with full-order flux observers. Publications III and IV consider mainly speed-sensored drives, but the methods and results are partially applicable to speed-sensorless drives. The scientific contribution is described in Section 5.2.

5.1 Abstracts

Publication I

This letter deals with voltage model flux estimators for sensorless induction motor drives. In order to eliminate the drift problems, the pure integrator of the voltage model is replaced with a first-order low-pass filter, and the error due to this replacement is compensated in a very simple way.

Publication II

This paper deals with the flux estimation for sensorless induction motor drives. Stable zero-speed operation is achieved by using a speed-adaptive full-order flux observer and a simple software compensation of inverter nonlinearities. No voltage feedback is needed for the compensation and hardware costs can be lowered. Experimental results including stable zero-speed operation are shown.

Publication III

This paper deals with flux estimation for induction motor drives by using a full-order flux observer. A problem of full-order flux observers is their need for computationally demanding discretization methods in order to work stably and accurately at high speeds. An implementation of the full-order flux observer using the stator and rotor fluxes as state variables in the stator reference frame and in the rotor reference frame, respectively, was recently proposed. This paper describes how an observer gain can be included in this structure. It is shown that discretization errors of the proposed implementation are small and that there is more freedom to choose an observer gain, even if the simple forward Euler discretization is used.

Publication IV

This paper deals with flux estimation for induction motor drives. The equations of the parameter sensitivity of both the rotor flux estimation and the torque production are derived for a full-order flux observer. Based on the parameter sensitivity analysis, practical methods of designing robust observer gains combining the current model and the voltage model are proposed. The proposed gains are easy to tune and lead to a simple observer structure. Experimental results show that for inaccurate parameter estimates, both the steady-state and dynamic errors in the produced torque are small as compared to the current model. Furthermore, high-speed operation is possible without modelling the magnetic saturation even if motor parameters are highly erroneous.

Publication V

This paper deals with the flux estimation for sensorless induction motor drives. The linearized model of the speed-adaptive full-order flux observer is applied to help choosing the observer gain and the speed-adaptation gains. It is shown that the linearized model reveals potential instability problems that are difficult to find by other means. An observer gain and a method to vary the speed-adaptation gains in the field-weakening region are proposed. Experimental results show stable operation in a very wide speed range.

Publication VI

This paper deals with the full-order flux observer design for speed-sensorless induction motor drives. An unstable region encountered in the regenerating mode at low speeds is well known. To remedy the problem, a modified speed-adaptation law is proposed. Instead of using only the current estimation error perpendicular to the estimated flux, the parallel component is also exploited in the regenerating mode. Using current estimation error loci in steady state, a linearized model, simulations, and experiments, it is shown that the observer using the proposed speed-adaptation law does not have the unstable region. It is also shown that the effect of erroneous parameter estimates on the accuracy of the observer is comparatively small.

Publication VII

In sensorless induction motor drives, flux estimators based only on the standard motor model work well at sufficiently high stator frequencies, but they fail at frequencies close to zero. To solve this problem, a new observer structure is proposed, combining a speed-adaptive full-order flux observer with a low-frequency signal-injection method. An error signal obtained from the signal-injection method is used as an additional feedback signal in the speed-adaptation law of the observer, resulting in a wide speed range, excellent dynamic properties, and zero-frequency operation capability. The enhanced observer is also robust against parameter errors. Experimental results are shown, including very slow speed reversals and long-term zero-frequency operation under rated load torque, as well as rated load torque steps and fast speed reversals under rated load torque.

5.2 Scientific Contribution

To the best of the author's knowledge, the main scientific contributions in the Publications concerning speed-sensorless flux estimation are:

- The enhanced version (3.7) of an algorithm by Shin et al. (2000) is proposed in Publication I.
- A computationally efficient digital implementation of full-order flux observers is proposed in Publication III. A similar idea has been previously applied to a different flux estimator by Jansen and Lorenz (1994). Another, even simpler digital implementation is given in the Appendix of Publication IV. A method of the same kind has been applied to computer simulations of ac motors by Niiranen (1999). The proposed implementations can also be applied to speed-adaptive full-order flux observers.
- In Publications IV and VI, the effects of parameter errors on the regenerating-mode operation are also analyzed. Previously, only the motoring-mode operation has been considered.
- The stability problems at higher speeds reported in Publication V have previously been unknown. The observer gain (3.44) and the method to vary the speed-adaptation gains in the field-weakening region are proposed. Furthermore, the unknown relationship between speed-adaptive full-order flux observers and the estimator by Schauder (1992) is clarified.
- The speed-adaptation law consisting of (3.36) and (3.45) stabilizing the regenerating mode at low speeds is proposed in Publication VI.
- The speed-adaptive full-order flux observer enhanced with the low-frequency signal-injection method by Leppänen and Luomi (2002) is proposed in Publication VII.

In this overview, stability problems of different flux estimators at low speeds are highlighted. Furthermore, the effect of parameter errors on the flux estimators described by Ohtani et al. (1992) and by Kubota et al. (1993) are shown to be similar.

Chapter 6

Conclusions

In this thesis, flux estimators for speed-sensorless induction motor drives were investigated. A basic requirement for any motor drive control is the stability. However, most speed-sensorless flux estimators proposed in the literature suffer from stability problems, even if the parameter estimates are accurate. Operation at low speeds (especially in the regenerating mode) is generally the most demanding working point of sensorless induction motor drives. Difficulties may also be encountered at higher speeds since sensorless flux estimators tend to become more sluggish, poorly damped, and even unstable. These problems are seldom discussed in the literature, probably because they can often be circumvented by considerably reducing the dynamic performance (bandwidths of the speed and flux controllers) at higher speeds. As discussed in this overview, the stability problems of inherently sensorless flux estimators and speed-adaptive flux estimators are very similar. Furthermore, there is a close resemblance between the effects of parameter errors on some inherently sensorless flux estimators and speed-adaptive flux estimators.

The problems both at low and high speeds are remedied in the speed-adaptive full-order flux observer design proposed in Publications V and VI. The observer gain is designed especially for nominal and high-speed operation. At low speeds in the regenerating mode, the conventional error term of the speed-adaptation law is modified. Furthermore, the effect of parameter errors on the proposed observer was shown to be comparatively small. The observer design achieves the goals outlined in Chapter 1, except that the robustness of the system at very low speeds may be insufficient. For example, long-term zero-frequency operation under load torque cannot be achieved in practice. To improve the robustness at low speeds, the speed-adaptive full-order flux observer can be augmented with a low-frequency signal-injection method as shown in Publication VII. The combination of the methods results in a robust system with fast dynamic response.

A suitable topic for future research is to investigate whether an on-line stator resistance estimator can be incorporated into the proposed flux observer design without impairing stability. It might also be possible to use the low-frequency signal-injection method to estimate the stator resistance.

Bibliography

Ambrožič, V., Nedeljković, D., and Nastran, J. (1999). "Sensorless control of induction machine with parameter adaptation." In *Proc. IEEE ISIE'99*, vol. 2, pp. 724–728, Bled, Slovenia.

Bauer, F. and Heining, H.-D. (1989). "Quick response space vector control for a high power three-level-inverter drive system." In *Proc. EPE'89*, vol. 1, pp. 417–421, Aachen, Germany.

Blaschke, F. (1972). "The principle of field orientation as applied to the new TRANSVEKTOR closed-loop control system for rotating-field machines." *Siemens Rev.*, **34**(5), pp. 217–220.

Bose, B. K. and Patel, N. R. (1997). "A programmable cascaded low-pass filter-based flux synthesis for a stator flux-oriented vector-controlled induction motor drive." *IEEE Trans. Ind. Electron.*, **44**(1), pp. 140–143.

Briz, F., Degner, M. W., and Lorenz, R. D. (2000). "Analysis and design of current regulators using complex vectors." *IEEE Trans. Ind. Applicat.*, **36**(3), pp. 817–825.

Briz, F., Diez, A., Degner, M. W., and Lorenz, R. D. (2001). "Current and flux regulation in field-weakening operation [of induction motors]." *IEEE Trans. Ind. Applicat.*, **37**(1), pp. 42–50.

Depenbrock, M. (1988). "Direct self-control (DSC) of invereter-fed induction machine." *IEEE Trans. Power Electron.*, **3**(4), pp. 420–429.

Ha, J.-I. and Sul, S.-K. (1999). "Sensorless field-orientation control of an induction machine by high-frequency signal injection." *IEEE Trans. Ind. Applicat.*, **35**(1), pp. 45–51.

Harnefors, L. (1997). *On analysis, control and estimation of variable-speed drives*. Ph.D. thesis, Dept. Elect. Power Eng., Royal Inst. Tech., Stockholm, Sweden.

Harnefors, L. (2001). "Design and analysis of general rotor-flux-oriented vector control systems." *IEEE Trans. Ind. Electron.*, **48**(2), pp. 383–390.

Harnefors, L., Jansson, M., Ottersten, R., and Pietiläinen, K. (2003). "Unified sensorless vector control of synchronous and induction motors." *IEEE Trans. Ind. Electron.*, **50**(1), pp. 153–160.

Harnefors, L. and Nee, H.-P. (1997). "Full-order observers for flux and parameter estimation of induction motors." In *Proc. EPE'97*, vol. 3, pp. 375–381, Trondheim, Norway.

Harnefors, L. and Nee, H.-P. (1998). "Model-based current control of AC machines using the internal model control method." *IEEE Trans. Ind. Applicat.*, **34**(1), pp. 133–141.

Hasegawa, M. and Matsui, K. (2002). "Robust adaptive full-order observer design with novel adaptive scheme for speed sensorless vector controlled induction motors." In *Proc. IEEE IECON'02*, vol. 4, pp. 83–88, Sevilla, Spain.

Hinkkanen, M. (2002a). "Analysis and design of full-order flux observers for sensorless induction motors." In *Proc. IEEE IECON'02*, vol. 4, pp. 77–82, Sevilla, Spain.

Hinkkanen, M. (2002b). "Method in connection with full-order flux observers for sensorless induction motors." *Int. Patent Applicat. PCT/FI2003/000775*, filed Oct. 18, 2002.

Hinkkanen, M., Leppänen, V.-M., and Luomi, J. (2003). "Flux observer enhanced with low-frequency signal injection allowing sensorless zero-frequency operation of induction motors." In *Conf. Rec. IEEE-IAS Annu. Meeting*, vol. 2, pp. 1150–1156, Salt Lake City, UT.

Hinkkanen, M. and Luomi, J. (2001). "Modified integrator for voltage model flux estimation of induction motors." In *Proc. IEEE IECON'01*, vol. 2, pp. 1339–1343, Denver, CO.

Hinkkanen, M. and Luomi, J. (2002). "Parameter sensitivity of full-order flux observers for induction motors." In *Conf. Rec. IEEE-IAS Annu. Meeting*, vol. 2, pp. 851–855, Pittsburgh, PA.

Hinkkanen, M. and Luomi, J. (2003). "Stabilization of the regenerating mode of full-order flux observers for sensorless induction motors." In *Proc. IEEE IEMDC'03*, vol. 1, pp. 145–150, Madison, WI.

Hoffmann, F. and Koch, S. (1998). "Steady state analysis of speed sensorless control of induction machines." In *Proc. IEEE IECON'98*, vol. 3, pp. 1626–1631, Aachen, Germany.

Hofmann, H. and Sanders, S. R. (1998). "Speed-sensorless vector torque control of induction machines using a two-time-scale approach." *IEEE Trans. Ind. Applicat.*, **34**(1), pp. 169–177.

Holtz, J. (1994). "Pulsewidth modulation for electronic power conversion." *Proc. IEEE*, **82**(8), pp. 1194–1214.

Holtz, J., Jiang, J., and Pan, H. (1997). "Identification of rotor position and speed of standard induction motors at low speed including zero stator frequency." In *Proc. IEEE IECON'97*, vol. 2, pp. 971–976, New Orleans, LA.

Holtz, J. and Quan, J. (2002). "Sensorless vector control of induction motors at very low speed using a nonlinear inverter model and parameter identification." *IEEE Trans. Ind. Applicat.*, **38**(4), pp. 1087–1095.

Holtz, J. and Quan, J. (2003). "Drift- and parameter-compensated flux estimator for persistent zero-stator-frequency operation of sensorless-controlled induction motors." *IEEE Trans. Ind. Applicat.*, **39**(4), pp. 1052–1060.

Hu, J. and Wu, B. (1998). "New integration algorithms for estimating motor flux over a wide speed range." *IEEE Trans. Power Electron.*, **13**(5), pp. 969–977.

Ide, K., Ha, J.-I., Sawamura, M., Iura, H., and Yamamoto, Y. (2002). "A novel hybrid speed estimator of flux observer for induction motor drives." In *Proc. IEEE ISIE'02*, vol. 3, pp. 822–827, L'Aquila, Italy.

Jansen, P. L. and Lorenz, R. D. (1994). "A physically insightful approach to the design and accuracy assessment of flux observers for field oriented induction machine drives." *IEEE Trans. Ind. Applicat.*, **30**(1), pp. 101–110.

Jansen, P. L. and Lorenz, R. D. (1995). "Transducerless position and velocity estimation in induction and salient AC machines." *IEEE Trans. Ind. Applicat.*, **31**(2), pp. 240–247.

Jansen, P. L. and Lorenz, R. D. (1996). "Transducerless field orientation concepts employing saturation-induced saliences in induction machines." *IEEE Trans. Ind. Applicat.*, **32**(6), pp. 1380–1393.

Kim, J., Nam, K., Chung, J., and Sunwoo, H. (2003). "Sensorless vector control scheme for induction motors based on a stator flux estimator with quadrant error compensation rule." *IEEE Trans. Ind. Applicat.*, **39**(2), pp. 492–503.

Kovács, K. P. and Rácz, I. (1959a). *Transiente Vorgänge in Wechselstrommaschinen, Band I*. Verlag der Ungarischen Akademie der Wissenschaften, Budapest, Hungary.

Kovács, K. P. and Rácz, I. (1959b). *Transiente Vorgänge in Wechselstrommaschinen, Band II*. Verlag der Ungarischen Akademie der Wissenschaften, Budapest, Hungary.

Kubota, H., Matsuse, K., and Hori, Y. (1997). "Behavior of sensorless induction motor drives in regenerating mode." In *Proc. IEEE PCC'97*, vol. 2, pp. 549–552, Nagaoka, Japan.

Kubota, H., Matsuse, K., and Nakano, T. (1993). "DSP-based speed adaptive flux observer of induction motor." *IEEE Trans. Ind. Applicat.*, **29**(2), pp. 344–348.

Kubota, H., Sato, I., Tamura, Y., Matsuse, K., Ohta, H., and Hori, Y. (2002). "Regenerating-mode low-speed operation of sensorless induction motor drive with adaptive observer." *IEEE Trans. Ind. Applicat.*, **38**(4), pp. 1081–1086.

Leonhard, W. (1996). *Control of Electrical Drives*. Springer, Berlin, Germany, 2nd edn.

Leppänen, V.-M. (2003). *Low-frequency signal-injection method for speed sensorless vector control of induction motors*. Ph.D. thesis, Dept. Elect. Commun. Eng., Helsinki Univ. Tech., Espoo, Finland.

Leppänen, V.-M. and Luomi, J. (2002). "Rotor flux angle tracking controller for sensorless induction motor drives." In *Conf. Rec. IEEE-IAS Annu. Meeting*, vol. 2, pp. 856–863, Pittsburgh, PA.

Maes, J. and Melkebeek, J. A. (2000). "Speed-sensorless direct torque control of induction motors using an adaptive flux observer." *IEEE Trans. Ind. Applicat.*, **36**(3), pp. 778–785.

Mitronikas, E. D., Safacas, A. N., and Tatakis, E. C. (2001). "A new stator resistance tuning method for stator-flux-oriented vector-controlled induction motor drive." *IEEE Trans. Ind. Electron.*, **48**(6), pp. 1148–1157.

Nelson, R. H., Lipo, T. A., and Krause, P. C. (1969). "Stability analysis of a symmetrical induction machine." *IEEE Trans. Power App. Syst.*, **PAS-88**(11), pp. 1710–1717.

Niiranen, J. (1999). "Fast and accurate symmetric Euler algorithm for electromechanical simulations." In *Proc. Elecrimacs'99*, vol. 1, pp. 71–78, Lisboa, Portugal.

Nitayotan, C. and Sangwongwanich, S. (2001). "A filtered back EMF based speed-sensorless induction motor drive." In *Conf. Rec. IEEE-IAS Annu. Meeting*, vol. 2, pp. 1224–1231, Chicago, IL.

Ohtani, T., Takada, N., and Tanaka, K. (1992). "Vector control of induction motor without shaft encoder." *IEEE Trans. Ind. Applicat.*, **28**(1), pp. 157–164.

Ottersten, R. and Harnefors, L. (2002). "Design and analysis of inherently sensorless rotor-flux-oriented vector control system." In *Proc. NORPIE/2002*, Stockholm, Sweden, CD-ROM.

Pedersen, J. K., Blaabjerg, F., Jensen, J. W., and Thogersen, P. (1993). "An ideal PWM-VSI inverter with feedforward and feedback compensation." In *Proc. EPE'93*, vol. 4, pp. 312–318, Brighton, U.K.

Peng, F.-Z. and Fukao, T. (1994). "Robust speed identification for speed-sensorless vector control of induction motors." *IEEE Trans. Ind. Applicat.*, **30**(5), pp. 1234–1240.

Peterson, B. (1996). *Induction machine speed estimation – observations on observers*. Ph.D. thesis, Dept. Ind. Elect. Eng. Automat., Lund Univ., Lund, Sweden.

Rashed, M., Stronach, F., and Vas, P. (2003a). "A new stable MRAS-based speed and stator resistance estimators for sensorless vector control induction motor drive at low speeds." In *Conf. Rec. IEEE-IAS Annu. Meeting*, vol. 2, pp. 1181–1188, Salt Lake City, UT.

Rashed, M., Stronach, F., and Vas, P. (2003b). "A stable MRAS-based sensorless vector control induction motor drive at low speeds." In *Proc. IEEE IEMDC'03*, vol. 1, pp. 139–144, Madison, WI.

Schauder, C. (1992). "Adaptive speed identification for vector control of induction motors without rotational transducers." *IEEE Trans. Ind. Applicat.*, **28**(5), pp. 1054–1061.

Schönung, A. and Stemmler, H. (1964). "Static frequency changers with "subharmonic" control in conjunction with reversible variable-speed a.c. drives." *Brown Boveri Rev.*, **51**(8/9), pp. 555–577.

Schroedl, M. (1996). "Sensorless control of AC machines at low speed and standstill based on the "INFORM" method." In *Conf. Rec. IEEE-IAS Annu. Meeting*, vol. 2, pp. 270–277, San Diego, CA.

Shin, M.-H., Hyun, D.-S., Cho, S.-B., and Choe, S.-Y. (2000). "An improved stator flux estimation for speed sensorless stator flux orientation control of induction motors." *IEEE Trans. Power Electron.*, **15**(2), pp. 312–318.

Slemon, G. R. (1989). "Modelling of induction machines for electric drives." *IEEE Trans. Ind. Applicat.*, **25**(6), pp. 1126–1131.

Suwankawin, S. and Sangwongwanich, S. (2002). "A speed-sensorless IM drive with decoupling control and stability analysis of speed estimation." *IEEE Trans. Ind. Electron.*, **49**(2), pp. 444–455.

Suwankawin, S. and Sangwongwanich, S. (2003). "Feedback gain assignment of an adaptive full-order observer for stabilization of speed-sensorless induction motor drives." In *Proc. EPE'03*, Toulouse, France, CD-ROM.

Tajima, H., Guidi, G., and Umida, H. (2002). "Consideration about problems and solutions of speed estimation method and parameter tuning for speed-sensorless vector control of induction motor drives." *IEEE Trans. Ind. Applicat.*, **38**(5), pp. 1282–1289.

Takahashi, I. and Noguchi, T. (1986). "A new quick-response and high-efficiency control strategy of an induction motor." *IEEE Trans. Ind. Applicat.*, **22**(5), pp. 820–827.

Tamai, S., Sugimoto, H., and Yano, M. (1987). "Speed sensor-less vector control of induction motor with model reference adaptive system." In *Conf. Rec. IEEE-IAS Annu. Meeting*, vol. 1, pp. 189–195, Atlanta, GA.

Teodorescu, R., Bech, M., Blaabjerg, F., and Pedersen, J. K. (2000). "Flexible drive systems laboratory – a modern teaching facility in electrical drives at Aalborg University." In *Proc. NORPIE/2000*, pp. 42–26, Aalborg, Denmark.

Tsuji, M., Chen, S., Izumi, K., and Yamada, E. (2001). "A sensorless vector control system for induction motors using q-axis flux with stator resistance identification." *IEEE Trans. Ind. Electron.*, **48**(1), pp. 185–194.

Verghese, G. C. and Sanders, S. R. (1988). "Observers for flux estimation in induction machines." *IEEE Trans. Ind. Electron.*, **35**(1), pp. 85–94.

Xu, X. and Novotny, D. W. (1991). "Implementation of direct stator flux orientation control on a versatile DSP based system." *IEEE Trans. Ind. Applicat.*, **27**(4), pp. 694–700.

Yang, G. and Chin, T.-H. (1993). "Adaptive-speed identification scheme for a vector-controlled speed sensorless inverter-induction motor drive." *IEEE Trans. Ind. Applicat.*, **29**(4), pp. 820–825.

HELSINKI UNIVERSITY OF TECHNOLOGY P.O. BOX 1000, FIN-02015 HUT http://www.hut.fi	ABSTRACT OF DOCTORAL DISSERTATION

Author Marko Hinkkanen

Name of the dissertation

Flux estimators for speed-sensorless induction motor drives

Date of manuscript 25th of August, 2004	Date of the dissertation 17th of September, 2004
☐ Monograph	☑ Article dissertation (summary + original articles)

Department	Department of Electrical and Communications Engineering
Laboratory	Power Electronics Laboratory
Field of research	Industrial electronics and electric drives
Opponent(s)	Prof. Frede Blaabjerg, Aalborg University, Denmark
Supervisor	Prof. Jorma Luomi, Helsinki University of Technology
(Instructor)	

Abstract

This thesis deals with flux estimators for speed-sensorless induction motor drives. To enhance the stability and the performance of state-of-the-art sensorless drives, new flux estimator designs based on the standard motor model are proposed. Theoretical and experimental research methods are both used. The dynamics and stability of flux estimators are analyzed using linearized models, and the effects of parameter errors are investigated using steady-state relations. Performance is evaluated using computer simulations and laboratory experiments. It was found that most sensorless flux estimation methods proposed in the literature have an unstable operating region at low speeds (typically in the regenerating mode) and that the damping at high speeds may be insufficient. A new stable design of the speed-adaptive full-order flux observer is proposed: the observer gain is designed especially for nominal and high-speed operation, while the low-speed operation is stabilized by modifying the speed-adaptation law. Compared to estimators proposed in the literature, the effects of parameter errors on the proposed observer design are shown to be small. To further improve the robustness, the speed-adaptive observer is enhanced with a low-frequency signal-injection method, allowing long-term zero-frequency operation under rated load torque. Furthermore, a computationally efficient version of a voltage-model-based flux estimator and two computationally efficient digital implementations for full-order flux observers are proposed.

Keywords Flux estimation, induction motor, sensorless control

UDC	Number of pages 46 + 55
ISBN (printed) 951-22-7188-5	ISBN (pdf) 951-22-7189-3
ISBN (others)	ISSN 1456-0445

Publisher Helsinki University of Technology, Institute of Intelligent Power Electronics

Print distribution Helsinki University of Technology, P.O. Box 3000, FIN-02015 HUT, Finland

☑ The dissertation can be read at http://lib.hut.fi/Diss/ 2004/isbn9512271893